Geological Society of America
Special Paper 302
1996

Geochemical comparison of four cores from the Manson impact structure

Randy L. Korotev, Kaylynn M. Rockow, Bradley L. Jolliff, and Larry A. Haskin
Department of Earth and Planetary Sciences and McDonnell Center for the Space Sciences, Washington University, St. Louis, Missouri 63130
Peter McCarville* and Laura J. Crossey
Department of Earth and Planetary Sciences, University of New Mexico, Albuquerque, New Mexico 87131

ABSTRACT

Concentrations of 33 elements were determined in relatively unaltered, matrix-rich samples of impact breccia at ~3-m-depth intervals in the M-1 core from the Manson impact structure, Iowa. In addition, 46 matrix-rich samples from visibly altered regions of the M-7, M-8, and M-10 cores were studied, along with 42 small clasts from all four cores. Major element compositions were determined for a subset of impact breccias from the M-1 core, including matrix-rich impact-melt breccia. Major- and trace-element compositions were also determined for a suite of likely target rocks.

In the M-1 core, different breccia units identified from lithologic examination of cores are compositionally distinct. There is a sharp compositional discontinuity at the boundary between the Keweenawan-shale-clast breccia and the underlying unit of impact-melt breccia (IMB) for most elements, suggesting minimal physical mixing between the two units during emplacement. Samples from the 40-m-thick IMB (M-1) are all similar to each other in composition, although there are slight increases in concentration with depth for those elements that have high concentrations in the underlying fragmental-matrix suevite breccia (SB) (e.g., Na, Ca, Fe, Sc), presumably as a result of greater clast proportions at the bottom margin of the unit of impact-melt breccia. The high degree of compositional similarity we observe in the impact-melt breccias supports the interpretation that the matrix of this unit represents impact melt. That our analyses show such compositional similarity results in part from our technique for sampling these breccias: for each sample we analyzed a few small fragments (total mass: ~200 mg) selected to be relatively free of large clasts and visible signs of alteration instead of subsamples of powders prepared from a large mass of breccia. The mean composition of the matrix-rich part of impact-melt breccia from the M-1 core can be modeled as a mixture of approximately 35% shale and siltstone (Proterozoic "Red Clastics"), 23% granite, 40% hornblende-biotite gneiss, and a small component (<2%) of mafic-dike rocks.

The SB unit is significantly different and more variable in composition than the IMB unit. Compared to the IMB in M-1, the SB is depleted in alkalis (K, Rb, Cs),

*Present address: 3867 Highway 92, Crawford, Colorado 81415.

Korotev, R. L., Rockow, K. M., Jolliff, B. L., Haskin, L. A., McCarville, P., and Crossey, L. J., 1996, Geochemical comparison of four cores from the Manson impact structure, *in* Koeberl, C., and Anderson, R. R., eds., The Manson Impact Structure, Iowa: Antomy of an Impact Crater: Boulder, Colorado, Geological Society of America Special Paper 302.

heavy rare-earth elements (Yb, Lu), and high field strength elements (Ta, Th, U). For many elements, the "transition zone" (TZ) between the IMB and the SB is intermediate in composition, corresponding roughly to a 2:1 mixture of SB and IMB. There is no compositional discontinuity at the TZ-SB boundary, but concentrations of some elements (e.g., Ca, Zn, and Cs) decrease discontinuously at the IMB-TZ boundary. We interpret the M-1 TZ as a physical mixing zone, perhaps formed by adjustment between the IMB and SB during uplift of the central peak.

Matrix-rich samples from IMB intervals in the other cores are generally similar in composition to those of the M-1 core; however, small but significant differences exist. Impact-melt breccias from the other cores are more variable in composition, in part because they have greater proportions of clasts. If the *melt* composition is the same for all cores, then the compositional differences among impact-melt *breccias* of different cores are caused largely by differences in the composition or abundance of clasts (plus some post-impact alteration effects) and the average composition of the clasts differs from that of the melt; this is most evident in M-7. Concentrations of Cs and Rb are significantly greater in the nonporous, relatively clast-poor IMB of M-1 than in the porous, clast-bearing or clast-rich IMB of the other cores. Concentrations of alkalis are also greater in the center of the IMB unit of M-1 than at the top and bottom of that unit. These observations suggest that alkalis were lost to hydrothermal fluids at the edges of the IMB unit of M-1 as well as from more porous IMB units elsewhere. The compositional characteristics of the M-1 TZ coupled with the fact that the TZ breccias have fragmental, porous matrices compared to the fairly impermeable overlying IMB suggest that the M-1 TZ may have been preferential for the flow of post-impact hydrothermal fluids. The different thicknesses of IMB units and variable mixing of IMB and SB indicated in the M-1, M-7, M-8, and M-10 cores reflect locally irregular thinning and adjustment of these units during central-peak uplift.

INTRODUCTION

The Manson impact structure (MIS), a well-preserved impact crater 36.5 km in diameter in northwestern Iowa, provides an opportunity to study the geochemical effects of a meteoroid impact into continental crust. We have studied samples of impactites from four drill cores, M-1, M-7, M-8, and M-10, which were each taken on the central uplift of the crater and which each intersected units identified as crystalline impact-melt breccia (Anderson et al., 1993; Roddy et al., 1994). We have also analyzed samples of crystalline target rocks from the Manson 2-A core (Hartung and Anderson, 1988) and sedimentary target rocks from the Amoco Eischeid No. 1 petroleum test well (Witzke, 1990; Koeberl and Hartung, 1992). The goals of our study are (1) to characterize and compare the compositions of the different breccia units identified during core logging (B. J. Witzke, unpublished) and in petrographic studies (e.g., Bell et al., this volume) and to establish a geochemical "stratigraphy," (2) to determine the composition of impact-melt breccias and the causes of any compositional variability, (3) to determine the source rocks of the impact melt and constrain their proportions, (4) to compare the composition of impact melt inferred from the M-1 impact-melt breccias to that of impact-melt veins in fractured basement rocks, and (5) to compare observations and results from the MIS with those for lunar breccias in order to help understand the complexity of the lunar breccias (e.g., Korotev, 1994; Rockow et al., 1994). This report is based mainly on compositional data obtained by instrumental neutron activation analysis (INAA) for trace elements and a few major elements on a large number of samples. We supplement these data with major element compositions determined by X-ray fluorescence (XRF) spectroscopy and electron microprobe analyses of fused beads (EMPA-FB) on a subset of the samples.

This work focuses mainly on "high-resolution" sampling and analysis of matrix-rich samples of the M-1 core. Our suite of samples from that core are minimally affected by alteration and constitute a representative set taken at closely spaced intervals (~3 m), thus allowing us to reliably delineate the geochemical stratigraphy. In contrast, our sampling of the M-7, M-8, and M-10 cores is less comprehensive as the samples were selected for a parallel study on post-impact alteration (McCarville and Crossey, this volume) and, thus, are deliberately biased in favor of altered samples.

Anderson et al. (1993) have described different breccia units in the M-1 core that are distinguished on the basis of clast lithologies and textures; similar units have been found and described in the other cores (Roddy et al., 1994). As a framework for discussion and comparison, we accept the units of

Anderson et al. (1993), but use unit designations consistent with other papers in this volume. For convenience, we will use acronyms such as IMB to refer specifically to *units* (not lithologies) described by Anderson et al. (1993) and Roddy et al. (1994).

In the system of Anderson et al. (1993), the uppermost breccia unit consists of clasts and blocks of shales, carbonates, siltstones, and sandstones set in a clastic matrix. This "sedimentary-clast breccia" (SCB) has been subdivided into a Phanerozoic-clast breccia (PCB, the upper subunit), and a Keweenawan-shale-clast breccia (KSCB, the lower subunit; Roddy et al., 1994). Similar breccias occur as the uppermost breccia units in cores M-8 and M-10, but because these are not yet well described in the literature, we refer generically to these units as "SCB" to indicate that they are breccias dominated by clasts of sedimentary rocks.

Below the KSCB, all breccias are dominated by clasts of crystalline rocks (the "crystalline-clast breccias" of Anderson et al., 1993). This region of the M-1 core has been divided into three major intervals or units (Anderson et al., 1993; Bell et al., 1993; this volume). (1) At the top is the impact-melt breccia (IMB), the unit that reached the highest temperature (Izett et al., 1993) and was most thoroughly melted. The IMB corresponds to "unit 1" of Bell et al. (1993; this volume) and the "crystalline-clast breccia with a melt matrix" ("CCB-M") of Anderson et al. (1993). (2) Below the IMB is the fragmental-matrix, suevite breccia (SB), which is similar to that described as "suevitic breccia," that is, a breccia having a clastic matrix with some melt clasts (Stöffler et al., 1979), or "melt-bearing mixed breccias" (Grieve et al., 1977). In referring to these rocks as "suevite breccia," we follow strictly the guidelines recommended by Stöffler and Grieve (1994) that impact breccias that have clastic matrix, but also contain melt or melt-breccia clasts, in any proportion, should be termed "suevite breccia." The M-1 SB corresponds to "unit 3" of Bell et al. (1993, this volume) and the "crystalline-clast breccia with a sandy matrix" ("CCB-S") of Anderson et al. (1993), because its matrix is dominantly fragmental. (3) Between the IMB and SB is a texturally intermediate unit known as the transition zone, TZ ("unit 2" of Bell et al., 1993, this volume). In the M-10 core, which has no IMB, there is a breccia unit with a matrix that is hybrid in nature between impact-melt and fragmental (Anderson, personal communication, 1995); that unit is designated IMB/SB here. Beneath the breccias are the crystalline rocks of the central peak, CPC ("central peak crystalline"; Anderson et al., 1993), which were sampled in the M-7 and 2-A cores. The crystalline rocks are mostly Early Proterozoic biotite and hornblende gneisses and Middle Proterozoic granite intrusives, with minor mafic intrusive rocks (Roddy et al., 1994). The crystalline rocks host veins that contain melt-like and finely brecciated material, possibly pseudotachylite (Anderson et al., 1993). Not all of these units were sampled or have been recognized in all of the cores.

The locations of contacts between units used in this chapter are those established and informally circulated by R. Anderson and coworkers at the Geological Survey Bureau of the Iowa Department of Natural Resources (GSB-IDNR). Sample depths are reported in feet because core logging and sample designations (e.g., M-1 516.7) have been based on depth in feet according to USGS core handling protocol.

SAMPLING AND ANALYSIS

Matrix-rich samples

Impact-breccia samples consisted of 1- to 4-g sections of core. After removing drilling scars and saw marks with a diamond-impregnated metal lap, we cleaned core sections by ultrasonification in deionized water (except for some samples of SCB, which were too friable) and drying them overnight at 85–90°C. A slice for thin sectioning was cut from each M-1 sample before cleaning. For our samples from SCB and SB units, clast sizes were commonly large, sometimes a significant fraction of the core diameter (4 cm) and some of our samples were too small to be representative of massive units of breccia. We wanted mainly to determine the composition of the matrix (the finer-grained material), so we employed the following subsampling strategy. We did not pulverize the samples, but crushed them coarsely with a steel piston mortar. After crushing, we ultrasonically cleaned the resulting fragments again so that clasts within the fragments were visible. We examined the fragments (1–3 mm) with a binocular microscope and selected only those fragments from each sample that appeared not to contain alteration veins or to be dominated by a few large clasts. Each analyzed subsample consisted of fragments totaling 100–200 mg in mass and, thus, represents a significantly smaller mass of material than for other studies of terrestrial craters in which analyzed subsamples represent tens of grams to several kilograms of powdered material (e.g., Floran et al., 1978; Reimold, 1982; Koeberl et al., this volume). The subsampling strategy and sample sizes used here, however, are the same as those typical of studies of lunar impact-melt breccias (e.g., Korotev, 1994). We analyzed each subsample "as-is" with no further grinding or dissolution. Thus, concentrations obtained by INAA are presented on a volatile-bearing basis, in contrast to concentrations obtained by EMPA-FB (below), which were obtained on fused samples. One subsample of each sample was analyzed, except that four subsamples each of four samples from the IMB unit of M-1 and three subsamples each of one compositionally anomalous sample from the IMB unit of M-8 were analyzed.

Clasts and target rocks

Because we wanted to compare compositions of clasts with those of matrix, we extracted 42 "small clasts" (3–20 mm) from the coarsely crushed samples of SB and IMB units for separate analysis. Analyzed masses ranged from 30 to 270 mg (median: 170 mg). A few of the small-clast samples were not single clasts; they consisted of several fragments of appearance similar to each other but dissimilar to the matrix-rich sample. For a few

clasts that were larger than about 0.3 g, the clasts were powdered and splits of the powder were analyzed. In order to obtain a better representation of the target rocks, we also took samples of some "large clasts" (~40 g to 200+ g) of crystalline rocks from the 2-A, M-1, and M-7 cores as well as samples of sedimentary rocks from three depths in the Eischeid drillhole. The Eischeid samples represent the lower units of the "Red Clastics" sequence of Proterozoic sediments that overlie the crystalline basement rocks (Witzke, 1990; Anderson and Hartung, 1992; Koeberl and Hartung, 1992). We dissected these samples to obtain representative splits for chemical analysis and thin sections. The splits for chemical analysis were cleaned as described above, crushed using a hydraulic splitter, and powdered and homogenized using a Spex™ shatterbox (alumina ceramic).

Trace elements

INAA procedures were similar to those described in Korotev (1991) except that all samples received an additional radioassay on the sixth day following irradiation for a total of three radioassays. In total, we obtained data for 33 elements in 149 subsamples of impact breccias and 67 subsamples of target rocks by INAA, although for Se, Br, W, Ir, and Au, concentrations were typically at or below detection limits. The data were obtained in five different batches (different neutron irradiations). The M-1 breccia data were all obtained in a single batch. With the M-1 batch of MIS samples, a single sample of USGS geochemical reference standard SDO-1 (shale, Devonian, Ohio) was run as a quality-control check (Table 1); our results agree well with the values recommended by Kane et al. (1990).

Major elements

For some samples from the IMB, TZ, and SB units of M-1, we ground some remaining clast-poor fragments in an agate mortar and pestle, fused the powders (5–15 mg) on a molybdenum strip heater, and analyzed the resulting glasses for major elements by EMPA. We prepared two or three beads from each powdered sample and analyzed 3–4 spots per bead using a JEOL 733 electron microprobe by wavelength-dispersive analysis. For standards, we used a combination of minerals and synthetic glasses. Analyses were done at 15 kV, ~30 nA, and ~30 μm beam diameter; results were monitored by frequent analyses of the glass standards. Concentrations of Na_2O were corrected for ~5% volatilization during fusion.

Using XRF spectroscopy, we analyzed major-element concentrations in a subset of the target-rock samples and two IMB samples from M-1 for which we had a sufficient mass of material (~1 g). We also analyzed two large clasts from IMB intervals (granite from M-1 and shale from M-7) and an apparent impact-melt-breccia dike from the M-7 CPC interval. Sample preparation and analysis procedures are described by Couture et al. (1993). Volatiles (mainly OH and CO_2) were estimated by loss on ignition (LOI).

RESULTS

Concentrations of elements determined by INAA for all samples of breccia matrix in the four cores are presented in Table A1.1 (Appendix 1) and profiles for 27 elements (and Rb/Cs and La/Yb ratios) are presented in Figure A1.1 (Appendix 1). Profiles for key elements in the IMB of the M-1 core are presented in Figure 1 and average compositions of units in M-1, as determined by INAA, are presented in Table 1. Major-element data for breccia samples are presented in Appendix 2 (Tables A2.1 and A2.2) and data for target rocks are presented in Appendix 3 (Tables A3.1–A3.3).

Comparison of units in M-1

The various core units distinguished during lithologic logging by the GSB-IDNR are compositionally distinct. In this section we describe the differences among the units for the M-1 core from top to bottom.

Phanerozoic-clast and Keweenawan-shale-clast breccias. Samples from the SCB (i.e., the PCB and KSCB) are highly variable in composition. These appear mostly to have light-gray clastic matrices with rather seriate clast size distributions and sharp contacts between clasts and matrix (macroscopically, we refer to aphanitic parts as matrix; under the petrographic microscope, we refer to material generally <20 μm as matrix). Our samples of these breccias are small and matrix-rich; macroscopically they appear to have some 10 to 25% clasts. Under the microscope, however, clasts (>30 μm) are more abundant. The clasts in these breccias represent a variety of compositionally distinct sedimentary lithologies (e.g., Bell et al., this volume; Koeberl et al., this volume), and the fine-grained clasts apparently derive from the same lithologies as the macroscopic clasts (Roddy et al., 1994). The compositional variability of these samples indicates that the matrix of these breccia intervals was not homogenized and local compositional variations reflect differences in compositions of original sedimentary components. Despite their compositional variability, our results show that, on average, the relatively fine grained portions of the SCB are significantly richer than the underlying IMB in elements that have high concentrations in limestone (Ca) and shales (As, Se, Sb) compared to most igneous rocks. They are also poorer than the IMB in elements that typically have higher concentrations in crystalline rocks consisting of plagioclase and mafic minerals than in sediments (e.g., Na, K, Sc, Cr, Fe, Ba). Profiles for these elements all show sharp discontinuities at the boundary between the KSCB and underlying IMB. Although absolute concentrations of Rb and Cs vary greatly, Rb/Cs ratios are relatively constant through the PCB and increase with depth through the KSCB to values like those of the underlying IMB. Relative concentrations of REE (rare earth elements) in the SCBs are similar to those of estimates of the average continental crust, but are enriched slightly in the middle REE (Sm, Eu, and Tb; Fig. 2).

There is only little evidence in our data for any compositional differences between the PCB and the KSCB. Concentra-

TABLE 1. RESULTS OF INAA FOR THE M-1 CORE AND CPC SAMPLES FROM M-7

	SDO-1*	SCB		IMB			TZ		SB		CPC	
		Mean†	s§	Mean**	s§	±‡	Mean§§	s§	Mean***	s§	Mean‡†	s§
wt. %												
Fe_2O_3(t)	9.26	4.22	2.12	5.65	0.26	0.06	7.37	0.48	6.88	0.80	11.40	0.82
CaO	1.16	11.2	5.8	2.9	0.6	0.3	3.3	0.6	5.3	1.6	6.4	0.7
Na_2O	0.37	0.42	0.37	3.16	0.24	0.03	4.19	0.33	4.50	0.17	4.11	0.22
K_2O	3.3	1.1	0.5	3.2	0.3	0.5	2.2	0.3	2.1	0.4	1.5	0.4
µg/g (except where indicated)												
Sc	12.91	6.89	0.97	12.81	0.49	0.13	15.10	1.49	16.51	1.78	22.9	2.6
Cr	66	44	3	58	7	0.6	85	17	102	25	92	15
Co	46.3	10.80	2.54	15.53	1.15	0.16	18.6	3.90	22.6	2.5	37.1	5.6
Ni	98	21	6	25	9	12	39	9	41	12	52	26
Zn	69	52	20	67	12	5	47	14	83	12	117	13
As	70	7.5	2.2	1.4	0.4	0.4	5.1	8.6	0.4	0.3	0.5	0.1
Se	1.7	0.3	0.2	<1		0.3	<1		<1		<1	
Br	4.1	0.5	0.2	0.5	0.3	0.3	0.2	0.1	0.4	0.2	1.3	0.4
Rb	126	41	20	119	9	2	75	8	66	12	44	7
Sr	80	201	77	236	23	14	267	53	393	35	382	39
Zr	132	213	33	210	26	16	151	16	135	42	292	50
Sb	4.4	0.45	0.11	0.14	0.04	0.02	0.12	0.08	0.03	0.01	0.03	0.02
Cs	6.7	2.03	1.34	1.86	0.17	0.03	1.13	0.17	0.99	0.12	0.60	0.14
Ba	380	141	55	661	28	12	692	39	751	81	716	69
La	37.1	25.3	4.1	33.3	1.6	0.4	30.3	1.2	27.6	5.4	45.1	4.7
Ce	75.8	53.4	7.3	68.3	2.7	0.7	61.4	1.0	56.7	10.8	95.5	9.9
Nd	33.8	24	4	30	1	2	27	2	26	5	47	5
Sm	7.98	5.07	0.58	6.49	0.22	0.07	5.72	0.19	5.41	0.66	10.02	0.90
Eu	1.61	1.08	0.15	1.29	0.06	0.02	1.23	0.09	1.31	0.13	2.66	0.20
Tb	1.15	0.69	0.10	1.03	0.06	0.02	0.80	0.07	0.74	0.07	1.34	0.14
Yb	3.43	2.15	0.26	3.93	0.22	0.05	2.58	0.32	2.37	0.19	3.57	0.24
Lu	0.50	0.32	0.04	0.58	0.03	0.01	0.38	0.04	0.35	0.03	0.52	0.04
Hf	4.67	5.63	0.73	5.94	0.51	0.06	4.13	0.33	3.90	0.90	6.86	0.74
Ta	0.92	0.86	0.08	1.65	0.47	0.05	1.27	0.43	0.91	0.23	1.03	0.04
W	1.24	0.8	0.1	<3	.....	0.8	<3	.....	<4	.....	1.7	0.6
Ir (ng/g)	0.0	0.2	0.2	0.0	0.1	0.8	0.3	0.4	0.3	0.4	0.3	0.7
Au (ng/g)	3.3	1.3	0.7	0.8	0.7	2	0.5	1.0	1.1	1.1	1.0	1.4
Th	9.68	6.43	0.87	10.18	1.01	0.12	8.30	1.21	6.98	2.68	5.30	0.55
U	49.0	3.0	0.26	7.1	1.0	0.3	5.0	1.7	4.8	1.1	2.7	0.4
Mass (g)	0.12	1.8	.....	3.8	.....	.....	0.8	.....	2.0	.....	0.8	.....

*Results of a single analysis of U.S.G.S. geochemical reference standard, SDO-1 (Devonian shale, Ohio).
†Mean for the 12 samples (206.45-335.5 feet) from the unit of sedimentary-clast breccia (SCB).
§Sample standard deviation of the values averaged for the previous column (most of the scatter results from sampling).
**Mean for samples from 11 depth intervals in the unit of impact melt breccia (IMB). Samples averaged include those between 358.7 and 459.25 feet, inclusive, i.e., the samples at 348 feet and 480 feet from near the boundaries with adjacent units were excluded from the mean. Also excluded was the highly anomalous sample at 470 feet. For those 4 depth intervals for which 4 subsamples each were analyzed (Table A1.1), results for the subsamples were averaged first, then the average for the different depth intervals was calculated.
‡Estimated analytical uncertainty (1 standard deviation) for a single analysis of a sample from the IMB unit.
§§Mean for the 5 samples (487.7-516.75 feet) from the transition zone unit (TZ).
***Mean for the 12 most typical samples (535.15-701.52 feet) from the unit of suevite breccia (SB)(i.e., 6 samples were excluded).
‡†Mean for the 5 samples of melt-breccia veins and dikes in the CPC unit of M-7.
INAA = instrumental neutron activation analysis.
Fe_2O_3 (t)= total Fe as Fe_2O_3.

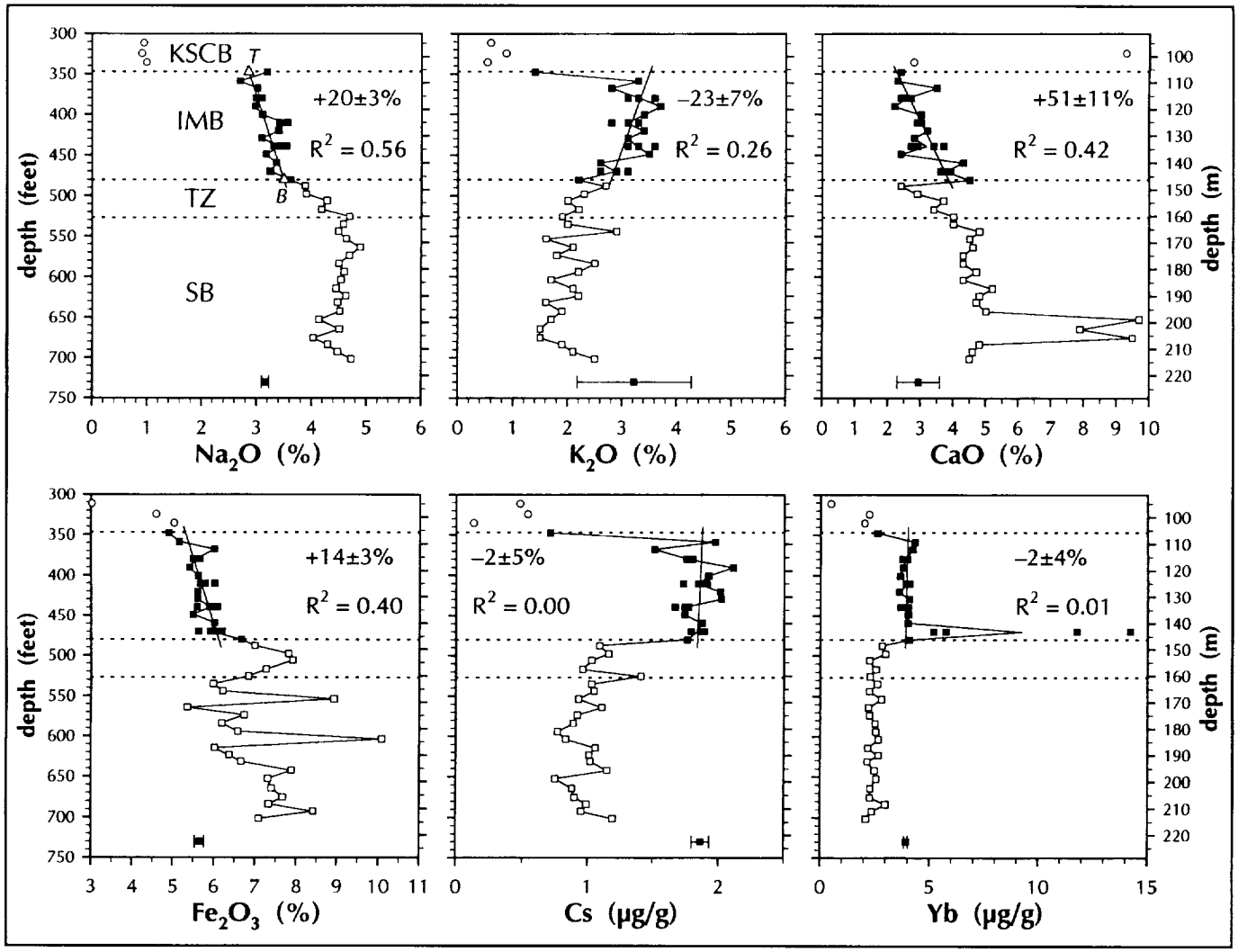

Figure 1. Profiles for six elements in the crystalline-clast breccias of core M-1. Filled squares = impact-melt breccia (IMB), and open squares = suevite breccia (SB) and transition zone (TZ). Samples from the Keweenawan-shale-clast breccia (KSCB) are represented by circles. The bar at the bottom of each plot represents ±2σ estimated analytical uncertainty for a typical sample with the composition of the M-1 melt breccia; the point is plotted at the mean concentration (C_M) of the IMB unit. (Compare uncertainty bar with the range of four subsamples at some depths in the IMB unit.) The diagonal lines represent least-squares regressions (R^2) of concentrations against depths for samples from the IMB units, with the top sample (347 ft) excluded (for Yb, the highly anomalous sample at 470 ft is also excluded from the regression). The slope of the line is stated in the figure as a percentage change from top (triangle *T* in Na_2O plot) to bottom (triangle *B*) of the IMB unit, with 95% confidence (±), i.e., $100(C_B-C_T)/C_M$, where C_B, C_T, and C_M are the concentrations at the top, bottom, and mean, respectively.

tions of Na are lowest while those of the other alkalis and Zn tend to be greatest in the PCB, although there is a distinct increase in the Rb/Cs ratio with depth through the KSCB.

Impact-melt breccia. In contrast to the SCB, matrix-rich portions of the 40-m-thick unit of impact-melt breccia (IMB) in M-1 are highly uniform in composition from sample to sample. For several elements (Sc, Fe, La, Eu), the sample standard deviation in the concentrations for samples from this unit are 5% or less of the concentration value (Table 1; Fig. 3). There is little evidence for physical mixing or chemical exchange between the IMB and the overlying SCB, except for one sample (347.7 ft; 106 m), which is within a foot of the contact, in which concentrations of some elements are intermediate (e.g., K, Rb, Cs, Zn, Ba, Sb, Eu, heavy REE). Bell et al. (this volume) note that clasts of sedimentary lithologies, although found throughout the IMB interval, are mainly restricted to the upper 1 m, consistent with

the composition of sample M-1 347.7. Bell et al. describe the upper 5.6 m of the IMB interval as having a relatively high fraction of very fine grained, mostly isotropic matrix; this and glassy textures, which we also see in our thin section of M-1 347.7, suggest more rapid cooling than the impact-melt breccias below, which developed coarser matrix textures. We see no significant compositional differences between samples M-1 358.7 and M-1 367.7, within and below, respectively, this upper "subunit" of the IMB interval.

Some individual samples within the IMB interval have anomalous concentrations of one or several elements, presumably as a result of small clasts of unusual composition, or vugs or veins containing alteration minerals. This is most evident in sample M-1 470.0 (four subsamples each), which is enriched in Ta, heavy REE (Fig. 1), U, and to a lesser extent, Hf and Th (probably due to sphene, which is present in thin section, but not obviously more abundant than in other samples). Some form of post-impact alteration may account for three consecutive samples that are enriched relative to the others in Br (M-1 380.05, 390.2, and 400.65), although we observe no unusual alteration features in our thin section of one of the samples (M-1 400.65).

A distinctive feature of the IMB unit of M-1 is its enrichment in alkali elements (K, Rb, and Cs), heavy REE (Tb, Yb, Lu), Ta, Th, and U compared to adjacent units (Figs. A1.1, 2). Concentrations of Cs in the IMB of M-1 are distinctly greater than in the overlying KSCB and underlying TZ and SB; they are also greater than those of the IMB or SB units of any of the other cores (see Fig. A1.1).

Transition zone. For all lithophile elements except perhaps Fe, the TZ is intermediate in average composition to the IMB and SB (Fig. A1.1). The high concentrations of Fe in the TZ may be either a sampling fortuity resulting from a few Fe-rich clasts in the analyzed samples or a mineralization effect associated with post-impact hydrothermal processes (below). The decrease in As and Sb concentrations from the IMB through the TZ and into the SB reflects the decrease in shale component with depth through the core. However, one of the five TZ sample (M-1 525.65) is highly enriched in As, Sb, and Se. Additional sampling and analysis is required to show whether this anomaly results from unrepresentative sampling associated with a large concentration of arsenopyrite in the analyzed sample or a more general mineralization process that affected this region of the breccia unit.

For most elements, there is no discontinuity in the concentration profile between the IMB and TZ. However, concentrations of some relatively immobile elements (heavy REE, Zr, and Hf) decrease discontinuously between the bottom of the IMB and the top of the TZ (i.e., between samples M-1 480.2 and 487.7). These discontinuities indicate that any gradation between the units occurs over less than 2.5 m and suggest differences in the proportions of components in the two breccia units. Concentrations of Ca, Sr, and Eu also decrease across the

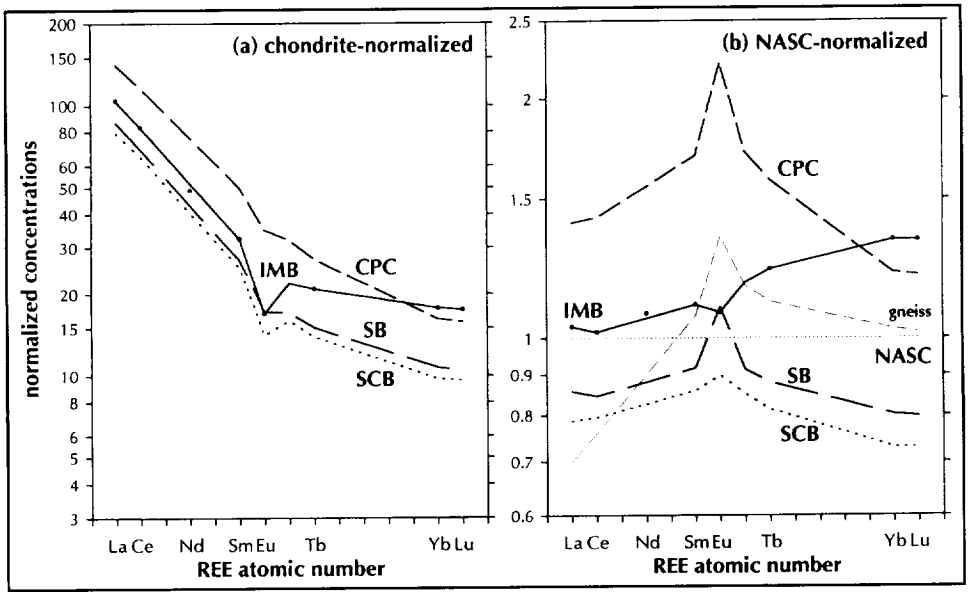

Figure 2. Average concentrations of rare earth elements (REE) in the veins and dikes of melt breccia from central-peak crystalline (CPC) rocks of M-7 and three breccia units from M-1. SCB, sedimentary-clast breccia, IMB, impact-melt breccia, and SB, suevite breccia. In (a), concentrations are normalized to ordinary chondrites (i.e., $1.36C_{CI}$, where C_{CI} is the concentration in "Mean C1 Chondr." of Anders and Grevesse, 1989). In (b), concentrations are normalized to the North American shale composite, an estimate of average continental crust (NASC, Gromet et al., 1984). The line labeled "gneiss" represents the average composition of 10 clasts of biotite/hornblende gneiss (Fig. 4). Only the elements labeled on the abscissa were analyzed; concentrations for other REE were estimated.

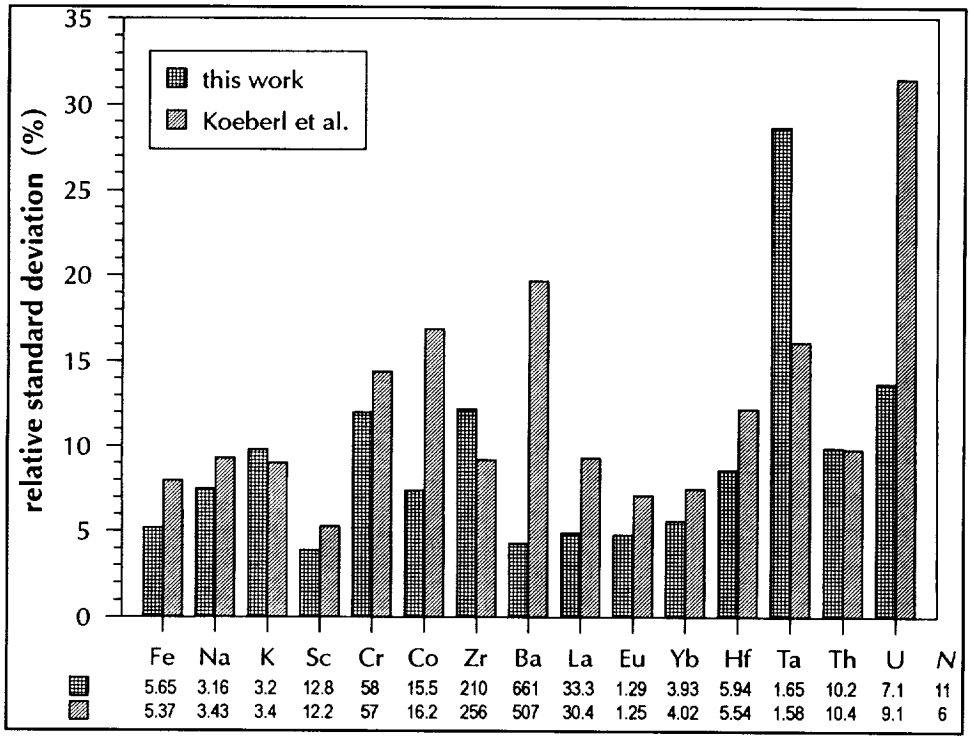

Figure 3. Comparison between this work (Table 1) and Koeberl et al. (this volume) of compositional dispersion among samples from the unit of impact-melt breccia in core M-1. The dispersion is indicated by the relative standard deviation (i.e., $s/\bar{x}$ (in percent), where s is the sample standard deviation and $\bar{x}$ is the mean of N samples). For both studies, results for all samples between 358 and 476 ft (109–145 m) were averaged, except that for "this work," the anomalous sample M-1 470.0 was excluded (Table A1) and for Koeberl et al. (this volume), the two anomalous samples from 415.0 ft were excluded. Thus, $N = 11$ for this work and $N = 6$ for Koeberl et al. (this volume). For comparison, values of $\bar{x}$ are tabulated under the element symbol (Fe, Na, and K as oxide percent, others as μg/g). For most elements, the strategy used in this work of analyzing a few small fragments (total mass: ~200 mg) selected to avoid large clasts and areas of obvious alteration is successful in yielding analyses with less dispersion than that of Koeberl et al. (this volume) in which several grams of core section ("about 5 to 15 cm in length") were powdered.

IMB-TZ boundary, and then gradually increase with depth through the TZ, suggesting some channelization of fluids and preferential dissolution or replacement of a Ca-bearing phase, probably plagioclase, just below the unit of impact-melt breccia. Circulation of hydrothermal fluids through the TZ, which is more porous than the IMB, may also account for the distinct decrease in Zn concentrations as well as some of the decrease in Cs concentrations in passing from the IMB to the TZ.

Suevite breccia. Samples from the SB are more variable in composition than those from the IMB, but are not as variable as samples from the PCB and KSCB. Six of the 18 analyzed samples are anomalous in that they are enriched in light REE (La, Ce), U, or elements associated with mafic phases (Fe, Sc, Cr, Co). Clasts with each of these characteristics were separated from samples of SB (Fig. 4). The mean of the remaining twelve samples is presented in Table 1. Relative abundances of the REEs in the SB are similar to those of the SCB, except that Eu is enriched (Fig. 2). Compared to the IMB, the SB is richer in elements associated with mafic phases (Fe, Sc, Cr, Co) and plagioclase (Ca, Na), but depleted in elements associated with shales (As, Sb) and granite (alkalis, heavy REE). This is consistent with the SB having a higher proportion of hornblende-rich gneiss in its precursor target suite of rocks (see Table A3.2) compared to the M-1 IMB.

Systematic variations with depth in the impact-melt breccia. Despite the compositional uniformity of the impact-melt breccia, there is slight systematic variation in the concentrations of some elements with depth.

Increased clast abundance with depth. Concentrations of elements that have high concentrations in the underlying SB (Na, Ca, Sc, Fe, and Sr) generally increase with depth through the IMB, whereas elements that have lower concentrations in the SB (K, As, and Sb) decrease (Figs. 1, A1.1). These trends, which for most elements continue through the TZ into the SB, are qualitatively consistent with the observed increase with depth within the IMB in the abundance of clasts of lithologies present

in the SB (Bell et al., 1993). Although the decrease in As and Sb is consistent with a decrease in the proportion of shale component with depth in the melt breccia, this decrease also results partly from dilution by As- and Sb-poor crystalline clasts. Mass-balance calculations suggest that compositional variations with depth in the IMB interval result mainly from incorporation of clasts of M-1 SB components; compositional variations related to clasts of KSCB-like components are of second-order importance and mostly involve those samples near the top of the M-1 IMB interval.

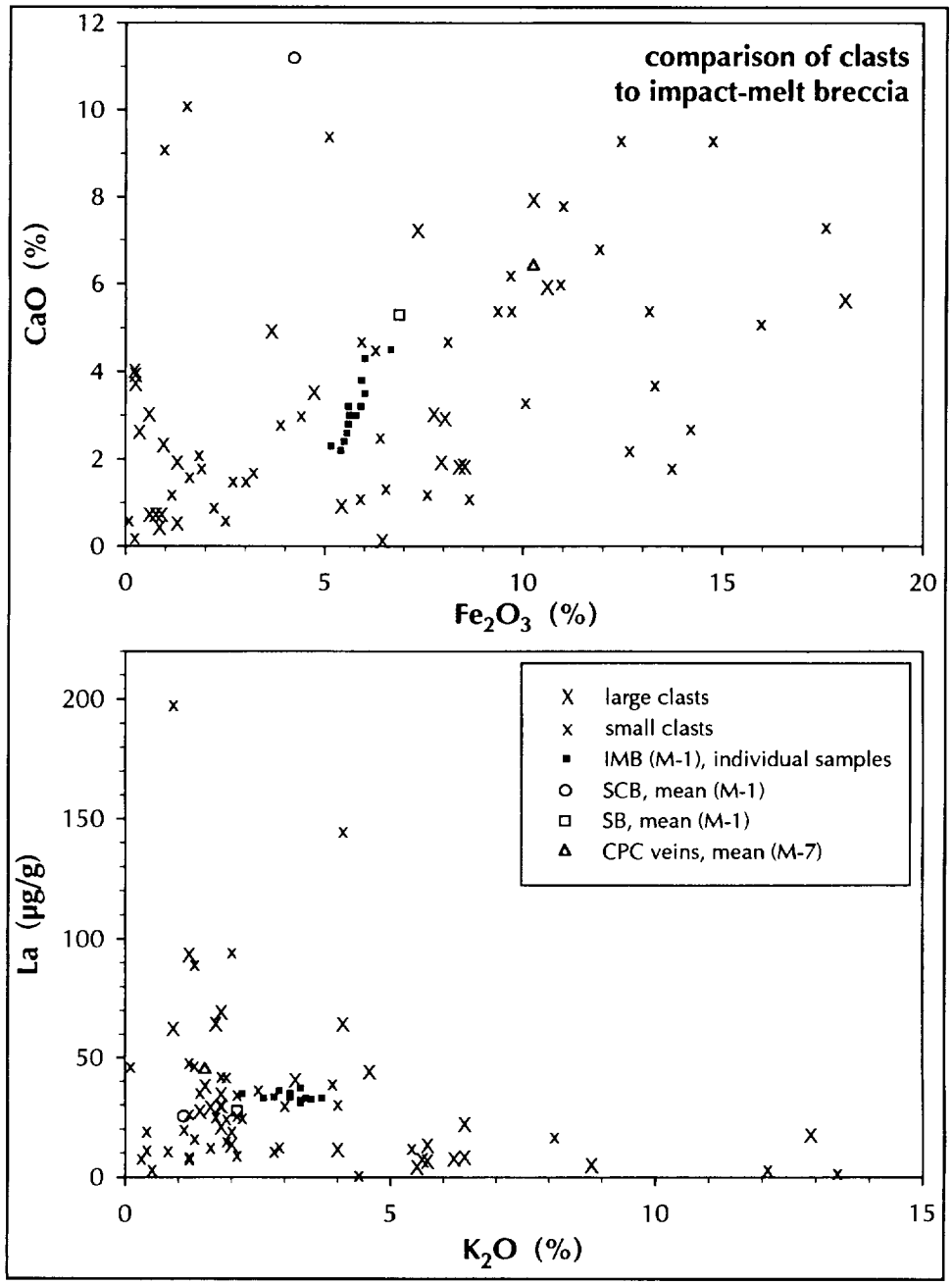

Figure 4. Comparison of clasts with the range of impact-melt-breccia (IMB) samples from M-1, and the means of the sedimentary-clast breccia (SCB) and suevite breccia (SB) units from M-1 and central-peak crystalline (CPC) melt veins from M-7 (means from Table 1). The "small clasts" (3–20 mm) were extracted from the same samples (1–4 g) as the matrix-rich subsamples from IMB and SB units plotted in Figure A1 (Appendix A). Most of the "large clasts" represent powdered subsamples prepared from 40- to 200-g samples of clastic blocks penetrated by the M-1, M-7, and 2-A cores. The clast lithologies have not all been identified, but many of the clasts with >7% Fe_2O_3 are biotite or hornblende gneisses and many of the clasts with <1% Fe_2O_3 are granites.

Alkali loss. Concentrations of the alkali elements K, Rb, and Cs are greater in the IMB unit than in other units of the core. However, within the IMB, the three elements each average about 20% greater in concentration at the center (380–430 ft; 115–131 m) than they do at the top (348–368 ft; 106–112 m) and bottom (439–480 ft; 134–149 m). These bow-shaped profiles are not observed for any other elements. The zone of highest alkali concentrations lies within the region of highest magnetic susceptibility (380–480 ft; 115–149 m), interpreted to be the hottest region of the melt unit (Izett et al., 1993). These observations suggest that there was some loss of alkalis from the top and, to a lesser extent, the bottom of the IMB unit. The sample with the most serious alkali loss is M-1 347.7, at the very top of the IMB unit.

Comparison of impact-melt breccias among the cores

Only in the M-1 core is a massive unit of fine-grained impact-melt breccia encountered. In the other cores the IMB units are thinner, more porous, and generally contain greater proportions of clasts, based on our observations of hand specimens and analysis of thin sections described in McCarville (1994). As a consequence, the IMB units of all four cores are similar to each other in composition to a first approximation, but in detail some important differences exist.

First, samples from the IMB of M-7, M-8, and M-10 are not as compositionally uniform as are those from M-1. Concentrations of Cs vary greatly among the six M-7 samples. One of the M-7 samples is significantly enriched in light REE and Eu (Fig. 5b) while one of the two M-8 samples (three subsamples each, near the SCB boundary) is highly anomalous, being depleted in "mafic" elements and enriched in incompatible trace elements. This lack of uniformity in the impact-melt breccias of the other cores presumably results from their higher clast abundances, lack of fine-grained matrix, and greater degree of post-impact alteration compared to the M-1 samples. Thus, the compositional variability may be caused at least in part by our deliberate selection (discussed above) of altered samples from the other cores. Clearly, a suite of representative, clast-poor, and minimally altered samples of melt breccia from cores M-7, M-8, and M-10 are needed for proper comparison to the IMB of M-1. Because of the small number and nonrepresentativeness of the IMB samples from core M-8 and M-10, we have not calculated an average IMB composition for these cores. The average composition of the IMB samples of core M-7 appears in Table 2.

Second, there are some systematic differences in *average* composition of the IMB units among the cores. In M-10, the unit of impact-melt breccia ("IMB/SB," Table A1.1) is hybrid in character between IMB and SB units observed in M-1, based on lithologic descriptions of cores (R. Anderson, personal communication, 1994). As a result, this unit is compositionally more similar to the TZ and SB than to the IMB of M-1, and the average composition corresponds reasonably well to a mixture of 2 parts IMB and 1 part SB from M-1. The large proportion of crystalline lithologies is sufficient to cause the relative REE abundances of the five samples from the IMB/SB of M-10 to differ significantly from that of M-1 (Fig. 5a,c).

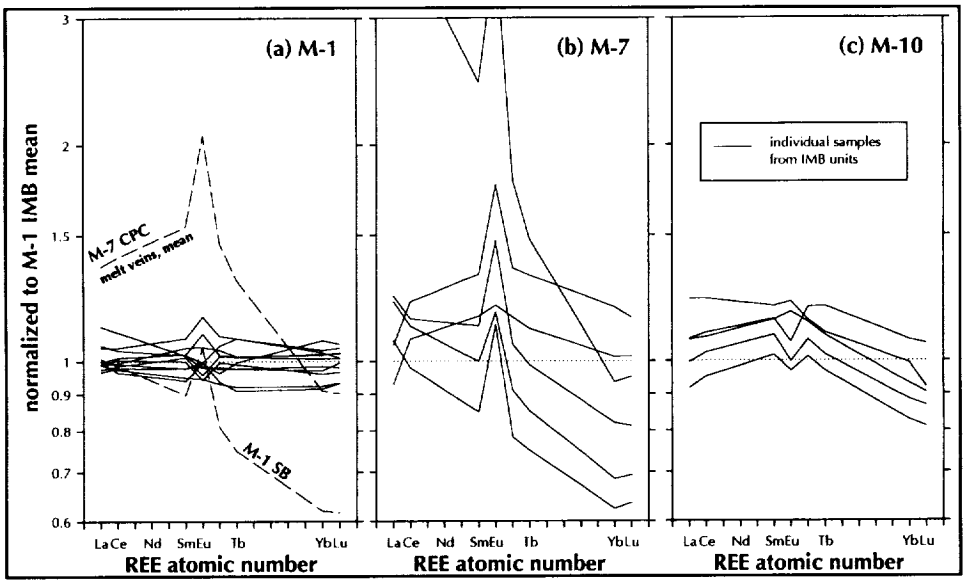

Figure 5. Comparison of REE concentrations in individual samples from IMB units of three cores (solid lines), normalized to mean concentrations in the M-1 core. (a) Individual samples from M-1 all have similar REE concentrations (the highly anomalous sample at 470 ft is not plotted). For reference, the mean concentrations in the SB unit of M-1 and the CPC dikes and veins from M-7 are also shown. (b) All M-7 samples contain a Eu-rich component and four of the six samples have a light-REE-rich component. (c) The M-10 samples all have REE "patterns" intermediate to the IMB of M-1 (dotted line) and the crystalline rocks (SB and CPC).

Similarly, the high clast abundance in the IMB in M-7 is the cause of the difference between the bulk composition of the IMB units in M-1 and M-7. Six of the "small clasts" (Fig. 4) were separated from the IMB of M-7. One of these clasts (clast C of Table 2) has highly fractionated REE (light REE and Eu enrichment) and, to varying degrees, this characteristic distinguishes four of the six samples of IMB from M-7 from the M-1 IMB (Fig. 5b). Ca and Fe concentrations are also lower, on average, in the IMB of M-7. A reasonably good match to the average composition of the IMB of M-7 can be obtained by mixing compositions of the IMB of M-1 with those of three of the clasts (rock type unknown) from the IMB of M-7 (Table 2). This model mixture is approximately a 50:50 mixture of M-1 IMB and clastic material, suggesting that the clast abundance in the IMB of M-7 is great.

Finally, the most significant difference among the cores is that Cs concentrations in the IMB unit of the other cores is only 40–70% as great as it is in M-1, and Rb concentrations are 65–85% as great. The IMB unit of M-1 is dense and fine grained, whereas IMB units of the other cores are more porous. These observations again suggest that the IMB unit in M-1 retained alkalis that were lost by other units in which higher porosity (McCarville, 1994) allowed hydrothermal dissolution of alkalis. As noted above, however, samples studied here from M-7, M-8, and M-10 were deliberately biased in favor of the altered and vein-bearing extreme of available material, whereas the M-1 samples were selected to be as free of alteration effects as possible. Thus, less altered samples of IMB from the other cores may have greater alkali concentrations than samples studied here. Another consideration is that if the impact-melt breccias in the other cores correspond to M-1-type melt-breccia matrix plus 50% or more additional clasts, and those clasts are not alkali-rich, then the clast load will effectively dilute the alkali elements, lowering their concentrations in the bulk breccia. However, even in the mass-balance example discussed above for the IMB of M-7 (Table 2), in which ~50% of the mixture is Cs-rich M-1 melt matrix (i.e., ~50% dilution), the Cs concentration of the best-fit mixture is still overestimated by 87%, suggesting that the *melt* component of the M-7 IMB has lost Cs.

Central peak melt veins. The five samples listed in Table A1.1 from the CPC unit of the M-7 core are small samples of veins and dikes of fine-grained melt breccia (in the generic, descriptive sense) within the CPC host rocks. In addition, we have analyzed another such sample, M-7 475.6, which appeared macroscopically to be very similar to typical impact-melt breccia, for both major and trace elements (Table A2.2). These samples are all compositionally more mafic (greater Ca, Fe, Sc, Cr, Co) than either the impact-melt breccias or the suevite breccias (Fig. 4). The six samples are all similar to each other in composition and to clasts of hornblende and biotite-bearing lithologies extracted from the suevite breccias (i.e., the "small clasts" of Fig. 4 with >7% Fe_2O_3) and hornblende-rich gneisses from the 2-A core (see Table A3.2). Sample M-7 475.6 also compositionally resembles a highly mafic diabase clast from the 2-A core (Table A3.2). Concentrations of some incompatible trace elements reach their highest average values in the CPC melt veins, with Zr and Hf concentrations being about a factor of 2 greater than in the SB and trivalent REE concentrations being 35 to 75% greater. Relative abundances of REEs are most similar to those of the hornblende-biotite gneisses (Fig. 2b) and are distinctly different from those of the impact-melt breccias, being enriched in Eu and depleted in heavy REE (Figs. 2, 5a). Curiously, Br concentrations are also greatest in the CPC melt veins.

TABLE 2. MODELING THE IMPACT-MELT BRECCIA IN M-7 AS A MIXTURE OF THE IMPACT-MELT BRECCIA IN M-1 AND CLASTS SUCH AS THOSE FOUND IN THE IMPACT-MELT-BRECCIA UNIT OF M-7

	Clast A	Clast B	Clast C	IMB	IMB	IMB
Core	M-7	M-7	M-7	M-1	M-7	M-7
Feet	223.45	182.0	194.9	Observed	Observed	Estimated
Lab id.	293.131	296.005	296.008	Mean	Mean	Model
Fraction %	23	15	10	52		100
wt. %						
Fe_2O_3	3.21	8.47	2.69	5.65	4.95	5.21
CaO	1.7	1.9	1.5	2.9	2.1	2.4
Na_2O	2.82	4.08	2.88	3.16	3.39	3.19
K_2O	3.9	2.0	2.0	3.2	2.8	3.1
µg/g (except where indicated)						
Sc	14.8	11.4	10.1	12.8	12.8	12.8
Cr	70.1	32.2	37.9	58.0	59.2	54.8
Co	7.5	31.2	6.7	15.5	14.6	15.1
Ni	12	40	10	25	30	23
Zn	33	204	75	67	85	80
As	1.1	9.5	3.7	1.4	1.9	2.8
Se	0.1	0.8	0.0	0.1	0.2	0.2
Br	0.38	0.20	0.78	0.52	0.45	0.47
Rb	147	72	71	119	102	113
Sr	200	220	200	236	240	221
Zr	160	170	260	210	186	197
Sb	0.20	0.13	0.41	0.14	0.22	0.18
Cs	4.96	0.57	1.46	1.86	1.25	2.34
Ba	694	535	430	661	680	626
La	39.1	19.3	94.5	33.3	36.5	38.6
Ce	74.7	49.3	171.0	68.3	75.5	77.1
Nd	32	25	70	30	32	34
Sm	6.17	6.23	11.45	6.49	7.06	6.87
Eu	1.46	1.51	3.07	1.29	1.73	1.54
Tb	0.80	0.99	1.38	1.03	1.04	1.01
Yb	2.57	3.24	4.35	3.93	3.40	3.55
Lu	0.397	0.486	0.664	0.578	0.497	0.530
Hf	4.65	4.71	7.88	5.94	5.07	5.64
Ta	1.26	0.77	0.88	1.65	1.48	1.35
W	1.2	1.6	1.1	0.8	1.3	1.1
Au (ng/g)	0.1	0.1	0.0	0.8	1.1	0.4
Th	9.05	8.73	8.41	10.18	9.05	9.51
U	5.9	5.5	3.7	7.1	4.9	6.2

Comparison of suevite breccias among the cores

The average compositions of SB units of M-7 and M-8 are more mafic than that of the SB of M-1. For example, concentrations of Fe_2O_3 average 9.5% (N = 13) and 9.9% (N = 4) for

M-7 and M-8, compared to 7.1% ($N = 18$) in M-1. Other differences occur, but because of the small mass and small number of samples and the large range in composition of the samples, these differences may not be significant.

Clasts and target rock samples

The suite of "small clasts" represents the clasts that were easiest to extract from the breccia samples; most are from suevite breccias, but some are from IMB or IMB/SB units of M-7, M-8, and M-10. The most commonly encountered small-clast type was biotite/hornblende gneiss (most of the high-Fe samples of Fig. 4), although shale, granite, diabase, pegmatitic granite (K-feldspar-rich), and sulfide-rich clasts were also recognized. Most of the "large clasts," including crystalline basement rocks from the 2-A core, were selected to obtain more representative samples of the coarse-grained target lithologies (e.g., granite, gneiss). Thus, the clast compositions (particularly for the small clasts) are not necessarily representative or typical compositions of the rock "units" from which the clasts derive. Likewise, the suite of lithologies represented by the clasts (both small and large) is not necessarily representative of the entire suite of target rocks of the MIS. Nevertheless, it is likely that each of the analyzed clasts represents a component of the impact melt. Thus, the small range in the composition of samples of the impact-melt breccia, compared to the range of the clasts, attests to the efficiency of the impact mixing process (Grieve et al., 1977; Phinney and Simonds, 1977; Floran et al., 1978; Reimold, 1982).

DISCUSSION AND INTERPRETATIONS

Uniformity of composition of M-1 IMB matrix-rich subsamples

Our data show that matrix-rich samples of impact-melt breccia (IMB unit) in the M-1 core are very similar in composition through more that 30 m of thickness. Macroscopically, the matrix-rich samples also appear very similar to each other (greenish-gray aphanitic matrix, clast bearing to clast rich, nonporous); however, microscopically they appear heterogeneous. At the scale of our analyzed samples (subcentimeter), the clast content is diverse, including mineral clasts and crystalline and sedimentary lithic clasts that are nonuniformly distributed. Thus, we find the compositional uniformity of the small samples to be quite remarkable.

It has been suggested that the matrix of the IMB unit is simply finely comminuted target rocks that has subsequently undergone recrystallization (Reagan et al., 1994, this volume). However, the overall compositional uniformity of the matrix-rich breccia samples, as well as various petrographic observations, support the interpretation that the matrix is, in fact, impact melt. Clasts generally have ragged, subrounded edges, reaction coronas, recrystallized margins, or are completely recrystallized. Microscopically, we observe clasts in variable states of partial digestion and reaction with matrix. Within a given sample and away from clasts where reaction halos occur, the truly fine grained matrix (less than ~20–30 μm) appears to be fairly uniform in texture. Matrix textures range from very fine grained, cryptocrystalline, and mostly isotropic to fine grained, devitrified or recrystallized, and intersertal or intergranular textures. In reflected light, matrix areas show a fairly uniform distribution of very fine grained, highly reflective, opaque mineral grains. All of these features are consistent with the matrix having originated as impact melt. As additional evidence that the IMB matrix (including many of the small quartz-rich clasts) represents impact melt (or "impact partial melt"), we observe granitic clasts in the impact-melt breccias that consist of partially melted feldspars and enclaves of recrystallized quartz. This is analogous to the very fine grained matrix in the IMB, which is enriched in feldspar components, and clasts in the IMB, which are enriched in quartz relative to any reasonable combination of target rocks (Reagan et al., this volume). We suggest that rather than preferential comminution, as suggested by Reagan et al. (1994), the feldspars were *preferentially melted.*

Our strategy of analyzing small fragments of breccia that appeared to be free of large clasts and alteration zones and that totaled only about 200 mg in mass was successful: the dispersion of our data among samples from the unit of impact-melt breccia is less for most elements than that obtained by homogenizing several grams of material (Fig. 3). Our compositional variations are also far less than variations observed by broad-beam EMP analyses of the fine-grained matrix in a given sample (e.g., Koeberl et al., this volume; Reagan et al., this volume; and our own unpublished data). This suggests that the material melted (or partially melted) by the impact, and consequently well mixed, was the source of many of the small, shocked quartz clasts and recrystallized quartz enclaves now found in the breccias. Other lithic and mineral clasts were subsequently entrained as the impact melt blasted through fragmented target rocks within the crater.

The compositional differences (Table 1, Table A2.2) between the melt-breccia veins in the CPC of M-7 and the IMB unit of M-1 seem to preclude the possibility that the veins are allochthonous impact melts, injected from the crater into the underlying fractured basement rocks. The compositional evidence strongly supports the contention of Anderson et al. (1993) that the veins and dikes are pseudotachylites formed locally by shearing and frictional melting within their host rocks. The relationship of these veins to their immediate host rocks warrants further study.

Origin and target-rock components of M-1 impact-melt breccia

Because the composition of the impact-melt breccia is distinct from that of the suevite breccia, the impact-melt breccia is not simply the equivalent of suevite breccia that achieved a higher temperature. The impact-melt breccia (in M-1, at least) contains components of both shale (or some combination of shale, siltstone, and sandstone) and granite in excess of that contained in the suevite breccia. The signature of the shale component is enrichment in chalcophile elements such as As and Sb and the signature of the granite component is enrichment in alkalis, Th, and U, compared to the SB and CPC samples. The depletion relative to trivalent REE of Eu in the impact-melt breccia compared to the suevite breccia and CPC samples also requires that the melt-matrix breccia contain a low-Eu component such as granite (Fig. 2a, Table 3).

We have used a least-squares mixing model (Boynton et al., 1975) to estimate the proportions of target rocks that combined to produce the impact melt as reflected by the mean composition of M-1 IMB matrix-rich samples. We have restricted our modeling to the major elements and the relatively nonvolatile trace elements. Using the components given in Table 3, the mass-balance calculations indicate that the composition of the IMB in M-1 is consistent with a mixture of approximately 35% lower "Red Clastics" (dominantly shale and siltstone), 23% granitic components, 40% gneissic components (dominantly hornblende-rich gneiss), and possibly a small component (<2%) of mafic-dike rocks.

We show results in Table 4 for specific mixing calculations using a variety of plausible components in different combinations. We include this table to illustrate the following point. Among the target rock types, there is substantial compositional variability on a scale exceeding the size of our samples (~50–300 g). This is especially evident for the different samples of "Red Clastics" from the Eischeid drillhole and the granites and gneisses from the 2-A core (Appendix 3). Still, we obtain fairly robust results for the different proportions of major categories of target rocks (i.e., "Red Clastics," granitic rocks, biotite-rich gneiss, hornblende-rich gneiss, and mafic-dike rocks). In Table 4b, we compare the compositions for two plausible model mixtures to the mean M-1 IMB composition. The agreement is good for most elements; however, model mixtures overestimate concentrations of volatile elements such as Zn, Sb, and Cs, suggesting loss of these elements from the superheated impact melt.

Differences among IMB, TZ, and SB units in core M-1: Implications for their origin

If the impact-melt breccia and suevite breccia had the same composition, that would suggest in-situ melting. Instead, however, the compositional differences between the IMB and SB units are consistent with formation of the two materials in separate regions of the target, followed by flow of the melt to the locations where it was sampled on the central peak (e.g., Bell et al., 1993). Other compositional evidence for flow is the increase in the compositional signature of mafic lithologies near the base of the IMB of M-1, presumably because of incorporation of clasts from the underlying SB. Compositionally, the transition zone appears to be a zone of physical mixing between suevite breccia and impact-melt breccia. The average composition of the TZ in M-1 corresponds to a mixture of roughly 2:1 SB:IMB, plus some 5% additional components such as Fe-sulfide and excess OH and silica components, perhaps related to interaction with hydrothermal fluid.

We suggest that the differences in composition between the IMB of M-1 and M-7 may result from differences in clast proportions and compositions, and that the *melt* matrix of these two cores may have the same composition. If the differences are, in fact, a consequence of greater clast proportions in the IMB of M-7, then the similarity in relative REE concentrations of the six M-7 samples to each other and their difference as a group from the M-1 samples (i.e., Eu and light REE enrichment; Fig. 5b) indicate that throughout the 16-m thickness of melt breccia in the M-7 core, a particular (but unidentified) microscopic clast lithology dominates, one that is not evident in M-1. This observation begs the general question of whether the matrix of each unit is compositionally the same as the integrated sum of its larger clasts. If not, a separate origin of clasts and matrix is indicated, as well as an additional process to put them together. We suggest that the differences between the impact-melt breccia of the M-1 core and the underlying suevite breccia reflect lateral movement perhaps related to flow of impact-melt breccia within the transient crater prior to central-peak rebound and, consequently, mixing at the contact between them, resulting in a transition or physical mixing zone. Differences between the IMB intervals of the M-1, M-7, M-8, and M-10 cores may result from locally variable readjustment of the IMB and SB units as the central peak rebounded.

ACKNOWLEDGMENTS

We appreciate the constructive reviews by B. Schuraytz and J. Blum of an early version of the manuscript. This work was supported by the National Aeronautics and Space Administration through grant NAGW-3343 (LAH) and DOE/BES grant DE-FG03-92ER14296 (LJC). Analytical costs were supported in part by the Department of Energy through Reactor Sharing grant DE-FG07-80ER10725 to the University of Missouri Research Reactor.

TABLE 3. COMPOSITIONS OF MANSON TARGET-ROCK COMPONENTS AND IMPACT BRECCIAS FOR MIXING ANALYSIS*

	SiO_2	TiO_2	Al_2O_3	Fe_2O_3	MnO	MgO	CaO	Na_2O
Eischeid C	57.5	1.08	16.6	7.61	0.06	4.70	1.46	1.74
Eischeid D	68.7	1.05	11.5	4.11	0.07	1.62	4.10	2.29
Eischeid E	83.3	0.35	7.2	2.51	0.03	0.43	1.31	0.79
Granite, average	74.2	0.09	13.2	0.87	0.02	0.49	1.80	3.55
M-1 Granite	74.7	0.06	12.7	1.47	0.02	0.98	0.66	2.97
Pegmatitic granite	69.4	0.09	15.0	1.23	0.01	0.23	2.43	2.64
Biotite gneiss	61.2	0.82	16.2	9.06	0.13	2.50	2.13	3.07
Hornblende gneiss	55.1	1.04	17.3	9.70	0.20	5.70	5.22	3.98
Hornblende-biotite gneiss	55.1	1.04	18.3	8.13	0.12	3.70	5.81	4.39
Mafic rocks	43.5	5.38	13.0	17.90	0.31	6.00	5.00	3.05
M-1 IMB top	63.8	0.82	15.2	5.20	0.10	3.50	2.70	2.80
M-1 IMB average	63.0	0.92	15.4	5.65	0.10	3.09	3.40	3.16
M-1 IMB bottom	61.3	1.03	16.0	6.10	0.10	3.00	4.00	3.45
M-1 TZ average	60.4	0.86	16.4	7.37	0.09	3.80	3.30	4.19
M-1 SB average	59.1	0.91	16.5	6.88	0.11	3.73	5.20	4.50
M-7 CPC average	55.0	0.80	14.0	11.40	0.15	5.00	6.42	4.11

	Zr	Sb	Cs	Ba	La	Sm	Eu	Yb
Eischeid C	177	3.48	6.9	430	37.0	8.35	1.50	4.14
Eischeid D	581	0.90	2.9	438	44.1	9.36	1.68	5.47
Eischeid E	126	0.82	1.7	453	20.2	4.51	0.95	2.34
Granite, average	97	0.04	1.0	547	11.1	2.31	0.81	1.08
M-1 Granite	234	0.14	0.8	451	12.9	3.86	0.38	2.79
Pegmatitic granite	29	0.03	1.0	947	42.5	7.67	1.01	0.89
Biotite gneiss	291	0.03	3.6	530	50.9	10.1	2.00	5.16
Hornblende gneiss	174	0.03	1.9	427	22.5	5.35	1.55	3.00
Hornblende-biotite gneiss	254	0.03	3.0	662	27.7	4.57	1.30	1.86
Mafic rocks	497	0.06	1.6	607	76.3	20.6	4.83	6.48
M-1 IMB top	215	0.16	1.9	670	32.0	6.40	1.27	4.00
M-1 IMB average	210	0.14	1.9	661	33.3	6.49	1.29	3.93
M-1 IMB bottom	205	0.09	1.7	652	35.0	6.80	1.40	3.80
M-1 TZ average	151	0.12	1.1	692	30.3	5.72	1.23	2.58
M-1 SB average	135	0.03	1.0	751	27.6	5.41	1.31	2.37
M-7 CPC average	292	0.03	0.6	716	45.1	10.0	2.66	3.57

TABLE 3. COMPOSITIONS OF MANSON TARGET-ROCK COMPONENTS AND IMPACT BRECCIAS FOR MIXING ANALYSIS* (continued)

	K_2O	P_2O_5	Sc	Cr	Co	Zn	Rb	Sr
Eischeid C	3.71	0.14	18.8	75	27.1	124	147	133
Eischeid D	2.83	0.24	10.0	37	9.0	70	90	156
Eischeid E	2.78	0.09	4.0	14	4.7	27	92	99
Granite, average	5.62	0.07	1.7	0.7	1.3	17	151	132
M-1 Granite	5.57	0.06	0.7	0.8	3.6	14	175	121
Pegmatitic granite	7.34	0.21	3.0	3.6	1.8	37	194	170
Biotite gneiss	2.38	0.12	19.4	60	11.1	148	110	177
Hornblende gneiss	1.62	0.26	32.7	120	35.8	181	71	336
Hornblende-biotite gneiss	1.76	0.26	17.2	54	21.1	127	72	537
Mafic rocks	1.40	2.50	29.8	39	45.3	181	32	293
M-1 IMB top	3.30	0.18	12.4	60	14.8	64	120	225
M-1 IMB average	3.10	0.21	12.8	58	15.5	67	119	236
M-1 IMB bottom	2.70	0.26	13.2	56	16.2	75	110	270
M-1 TZ average	2.40	0.17	15.1	85	18.6	47	75	267
M-1 SB average	2.00	0.20	16.5	102	22.6	83	66	393
M-7 CPC average	1.54	0.15	22.9	92	37.1	117	44	382

	Hf	Ta	Th	Ca/Al	Na/K	Rb/Cs	Zr/Hf	La/Yb
Eischeid C	5.65	1.1	12.6	0.12	0.42	21	31	8.9
Eischeid D	15.3	1.1	11.6	0.48	0.72	31	38	8.0
Eischeid E	3.72	0.4	4.5	0.25	0.25	54	34	8.6
Granite, average	3.49	0.4	12.4	0.18	0.56	157	28	10.3
M-1 Granite	8.86	0.5	32.5	0.07	0.48	224	26	4.6
Pegmatitic granite	1.17	0.5	36.6	0.22	0.32	196	25	47.8
Biotite gneiss	7.85	1.4	12.8	0.18	1.15	31	37	9.9
Hornblende gneiss	3.59	1.2	2.7	0.41	2.20	37	48	7.5
Hornblende-biotite gneiss	6.06	0.8	3.7	0.43	2.23	24	42	14.9
Mafic rocks	12.1	1.7	5.4	0.52	1.95	20	41	11.8
M-1 IMB top	5.70	1.7	9.0	0.24	0.76	65	38	8.0
M-1 IMB average	5.94	1.6	10.2	0.30	0.91	64	35	8.5
M-1 IMB bottom	6.10	1.6	12.5	0.34	1.14	63	34	9.2
M-1 TZ average	4.13	1.3	8.3	0.27	1.56	66	37	11.7
M-1 SB average	3.90	0.9	7.0	0.43	2.01	67	35	11.6
M-7 CPC average	6.86	1.0	5.3	0.62	2.39	74	43	12.6

*Average compositions estimated from X-ray fluorescence (XRF), electron microprobe analysis of fused beads (EMPA-FB), and instrumental neutron activation analysis (INAA) data. Average compositions of crystalline rocks include compositions of many clasts extracted from breccias. Compositions of the "Red Clastic" sedimentary components are of samples from the Eischeid drillhole (Table A6). The composition of "M-1 Granite" is that of sample M1 355.9 granite clast in the impact-melt-breccia interval (Table A4). The composition of "Hornblende-biotite gneiss" is the average shown in Table A5. The major-element compositions of "M-1 IMB average," "TZ average," and "SB average" are derived from XRF and EMPA-FB data contained in Tables A2 and A3; the trace-element compositions are from Table 1. Compositions of impact-melt breccias at the top and bottom of the IMB interval in the M-1 core were estimated from trends on compositional profiles. Abbreviations: IMB = impact-melt breccia; TZ = transition zone between IMB and SB intervals; SB = fragmental-matrix, suevitic breccia; CPC = central-peak crystalline rocks.

TABLE 4A. MIXING-MODEL RESULTS FOR THE M-1 IMPACT-MELT PROPORTIONS OF TARGET ROCKS MELTED*

Mix Component	(1)	(2)	(3)	(4)	(5)	(6)	(7)	(8)	(9)	(10)	(11)	(12)	(13)	Min.	Avg.	Max.	St. Dev. (N-1)
Eischeid E												—	1.5				
Eischeid D	27.1	24.7	19.2	19.1	28.0	24.0	18.2	17.9	18.5	18.2	19.7	16.8	16.5				
Eischeid C	8.4	5.3	23.7	23.4	2.7	-4.0	22.2	21.6	21.4	19.6	21.3	13.1	12.6				
Red Clastics Sum	**35.5**	**30.0**	**43.0**	**42.5**	**30.7**	**20.0**	**40.4**	**39.5**	**40.0**	**37.8**	**41.0**	**29.9**	**30.6**	**20.0**	**35.4**	**43.0**	**6.8**
Average granite	24.3	27.8	18.4	18.8							19.8						
M-1 Granite clast					26.4	32.9	19.1	19.7	19.4	20.8		16.2	16.3				
Pegmatitic granite												6.9	6.6				
Granite Sum	**24.3**	**27.8**	**18.4**	**18.8**	**26.4**	**32.9**	**19.1**	**19.7**	**19.4**	**20.8**	**19.8**	**23.1**	**22.9**	**18.4**	**22.6**	**32.9**	**4.3**
Biotite Gneiss	**11.4**	**9.6**	**6.6**	**6.5**	**7.5**	**4.2**	**2.8**	**2.5**	**2.9**	**2.5**	**6.6**	**5.5**	**5.4**	**2.5**	**5.7**	**11.4**	**2.8**
Hornblende gneiss	27.4	26.6			34.1	34.7			1.4	2.7	3.3	8.1	8.3				
Horn-bio gneiss			30.9	30.8			36.6	36.5	35.2	33.9	27.2	28.1	28.1				
Hornbld Gneiss Sum	**27.4**	**26.6**	**30.9**	**30.8**	**34.1**	**34.7**	**36.6**	**36.5**	**36.6**	**36.6**	**30.5**	**36.2**	**36.4**	**26.6**	**33.4**	**36.6**	**3.7**
Gneiss Sum	**38.9**	**36.2**	**37.5**	**37.2**	**41.6**	**38.8**	**39.4**	**39.1**	**39.5**	**39.1**	**37.2**	**41.6**	**41.8**	**36.2**	**39.1**	**41.8**	**1.8**
Mafic dike		3.2		0.2		4.7		0.4		0.7	0.5	1.8	1.8	0.3	1.7	4.7	1.6
Total	**98.7**	**97.2**	**98.8**	**98.7**	**98.7**	**96.5**	**98.9**	**98.7**	**98.9**	**98.5**	**98.5**	**96.4**	**97.0**				
χ^2/ν	5.8	5.8	3.9	4.3	8.4	8.1	5.0	5.4	5.4	5.9	4.5	5.8	6.4				

*Mixing based on 18 elements, including Si, Ti, Al, Fe, Mg, Ca, Na, K, Sc, Co, Zr, La, Sm, Eu, Yb, Hf, Ta, Th. The "Eischeid E" component is a red, arkosic sandstone, "Eischeid D" is a red mudstone (silty shale), and "Eischeid C" is a black shale (see Table A6). χ^2/ν = reduced chi-square: error-weighted sum of squares of residuals divided by the number of degrees of freedom (number of elements minus number of components; e.g., Boynton et al., 1975). The magnitude of χ^2 depends on specific weighting factors, thus, as used here, χ^2/ν is simply a measure of the relative goodness of fit among the mixes shown above. The combinations shown are the best mixes obtained using these components. Other combinations of components are possible, but those not shown are either much poorer fits or involve substantial negative values for one or more components. For example, the "Eischeid-E" component is negative in most mixes that include it. The averages and standard deviations for the main categories of components are shown to illustrate that although there is substantial variability in the proportions of components depending on how they are combined in the model and on which of the specific granitic and gneissic components are used, the proportions shown in bold are fairly robust. In the two examples given below, the mixing-model compositions match quite well for the less volatile and less mobile elements. The volatile elements Cs and Sb, for example, are depleted in the impact-melt relative to the modeled mixtures of target rocks.

TABLE 4B. MIXING-MODEL RESULTS: COMPOSITIONS OF TWO EXAMPLES OF RELATIVELY GOOD FITS

	M-1 IMB Mean	Mix #10	Mix #11		M-1 IMB Mean	Mix #10	Mix #11		M-1 IMB Mean	Mix #10	Mix #11		M-1 IMB Mean	Mix #10	Mix #11
SiO_2	63.0	61.3	61.6	K_2O	3.10	3.11	3.16	Zr	210	291	268	Hf	5.94	8.17	7.26
TiO_2	0.92	0.86	0.86	P_2O_5	0.21	0.20	0.19	Sb	0.14	0.89	0.94	Ta	1.65	0.86	0.88
Al_2O_3	15.4	15.2	15.1	Sc	12.8	13.1	13.5	Cs	1.9	3.2	3.3	Th	10.2	13.0	9.4
Fe_2O_3	5.65	5.93	5.84	Cr	58	45	46	Ba	661	512	519	Ca/Al	0.30	0.30	0.30
MnO	0.10	0.08	0.08	Co	15.5	16.5	15.8	La	33.3	29.8	30.9	Na/K	0.91	0.88	0.87
MgO	3.09	2.94	2.81	Zn	67	93	95	Sm	6.49	6.25	6.29	Rb/Cs	64	35	33
CaO	3.40	3.37	3.40	Rb	119	111	108	Eu	1.29	1.25	1.38	La/Yb	8.5	9.1	9.8
Na_2O	3.16	3.07	3.07	Sr	236	277	256	Yb	3.93	3.28	3.16	Zr/Hf	35.3	35.6	37.0

APPENDIX 1. INAA DATA FOR IMPACT BRECCIA SAMPLES: ELEMENT CONCENTRATION PROFILES AND DATA TABLE

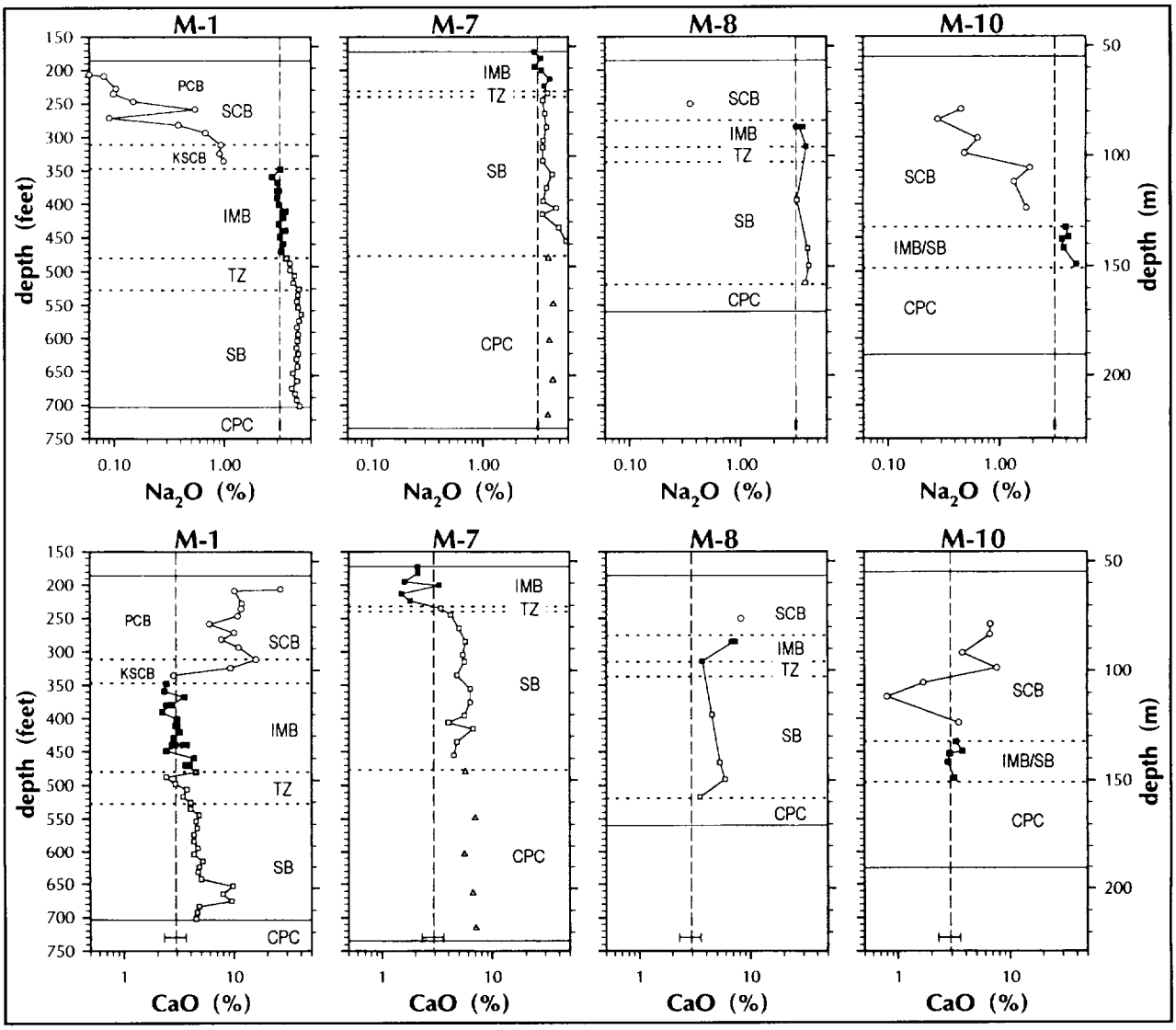

Figure A1.1 (on this and following nine pages). Element concentration and ratio profiles; see Figure 1. In M-7, the triangles represent samples of veins and dikes of melt breccia within the central-peak crystalline (CPC) rocks. The solid horizontal lines indicate the boundaries of recovered core material; the dashed horizontal lines indicate boundaries between recognized units. (SCB = sedimentary-clast breccia, which includes the PCB [Phanerozoic-clast breccia] and KSCB [Keweenawan-shale-clast breccia], IMB = impact melt breccia, TZ = transition zone, SB = suevite breccia, and CPC = central-peak crystalline. For reference, the dashed vertical line in each plot is the average composition of the IMB unit of core M-1 (Table 1). Unlike Figure 1, concentration axes of most plots are logarithmic and have the same scale for all plots. Linear axes are used only for Br, Au, and Ir, for which concentrations of most samples are below the detection limits. Samples that fall on the left border of a plot (e.g., As, Se, Sb) are at or below the concentration value represented by the left border.

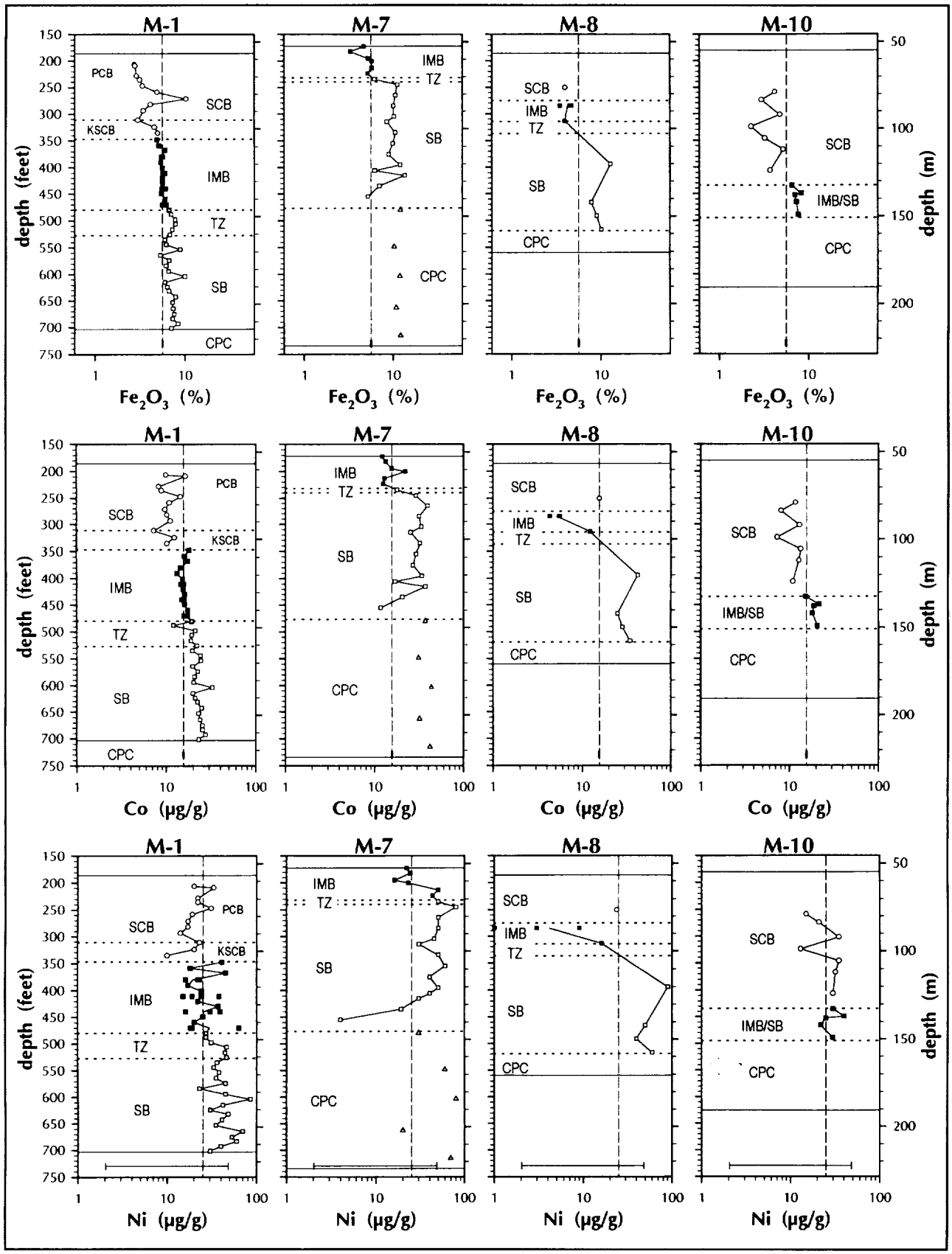
M-1
M-7
M-8
M-10
depth (feet)
depth (m)
PCB
SCB
KSCB
IMB
TZ
SB
IMB/SB
CPC
Fe2O3 (%)
Co (µg/g)
Ni (µg/g)

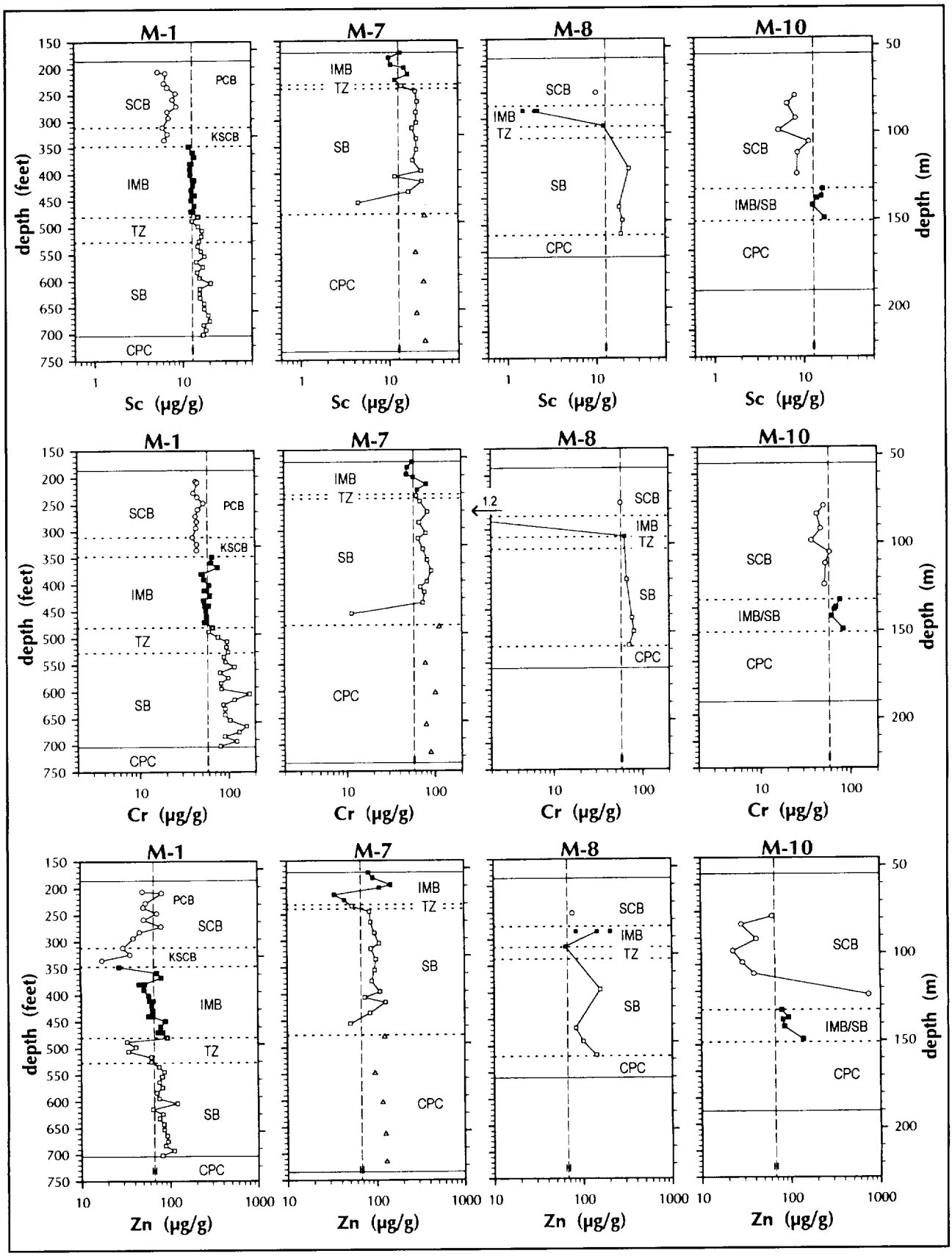
M-1
M-7
M-8
M-10
depth (feet)
depth (m)
PCB
SCB
KSCB
IMB
TZ
SB
CPC
IMB/SB
Sc (µg/g)
Cr (µg/g)
Zn (µg/g)
1.2

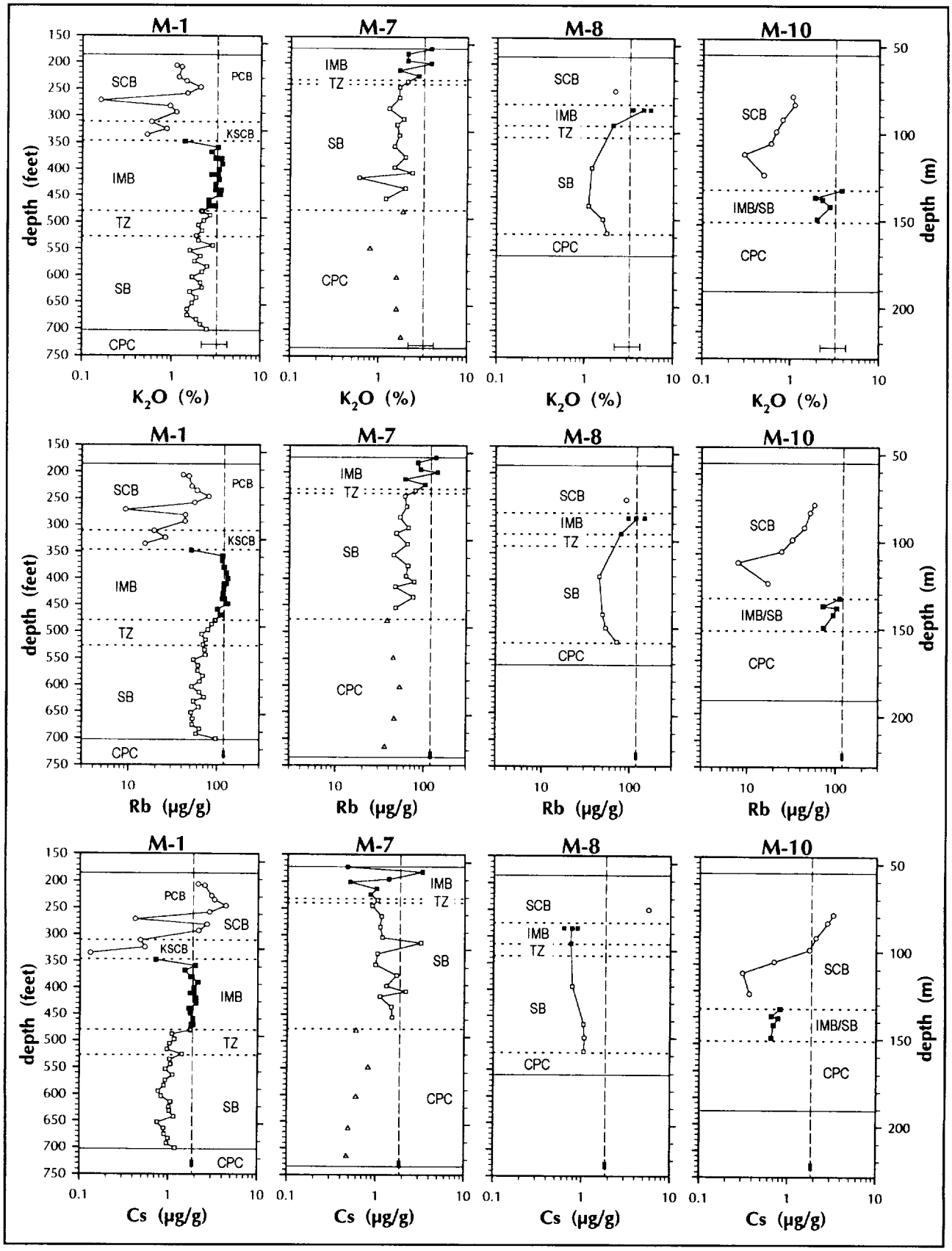
M-1
M-7
M-8
M-10
depth (feet)
depth (m)
SCB
PCB
KSCB
IMB
TZ
SB
IMB/SB
CPC
K_2O (%)
Rb (μg/g)
Cs (μg/g)

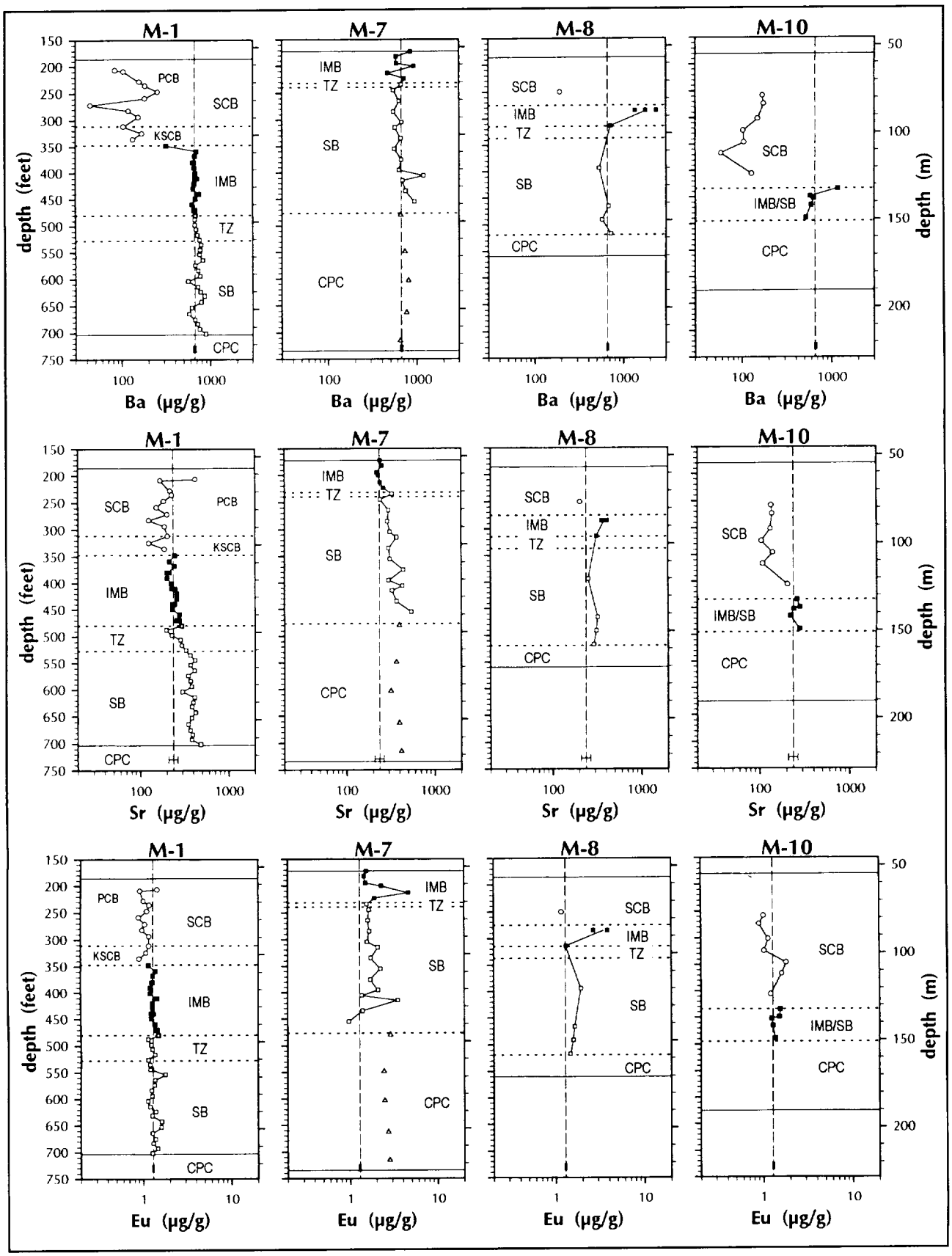
M-1
M-7
M-8
M-10
depth (feet)
depth (m)
PCB
KSCB
SCB
IMB
TZ
SB
IMB/SB
CPC
Ba (µg/g)
Sr (µg/g)
Eu (µg/g)
100
1000
1
10
150
200
250
300
350
400
450
500
550
600
650
700
750
50
100
150
200

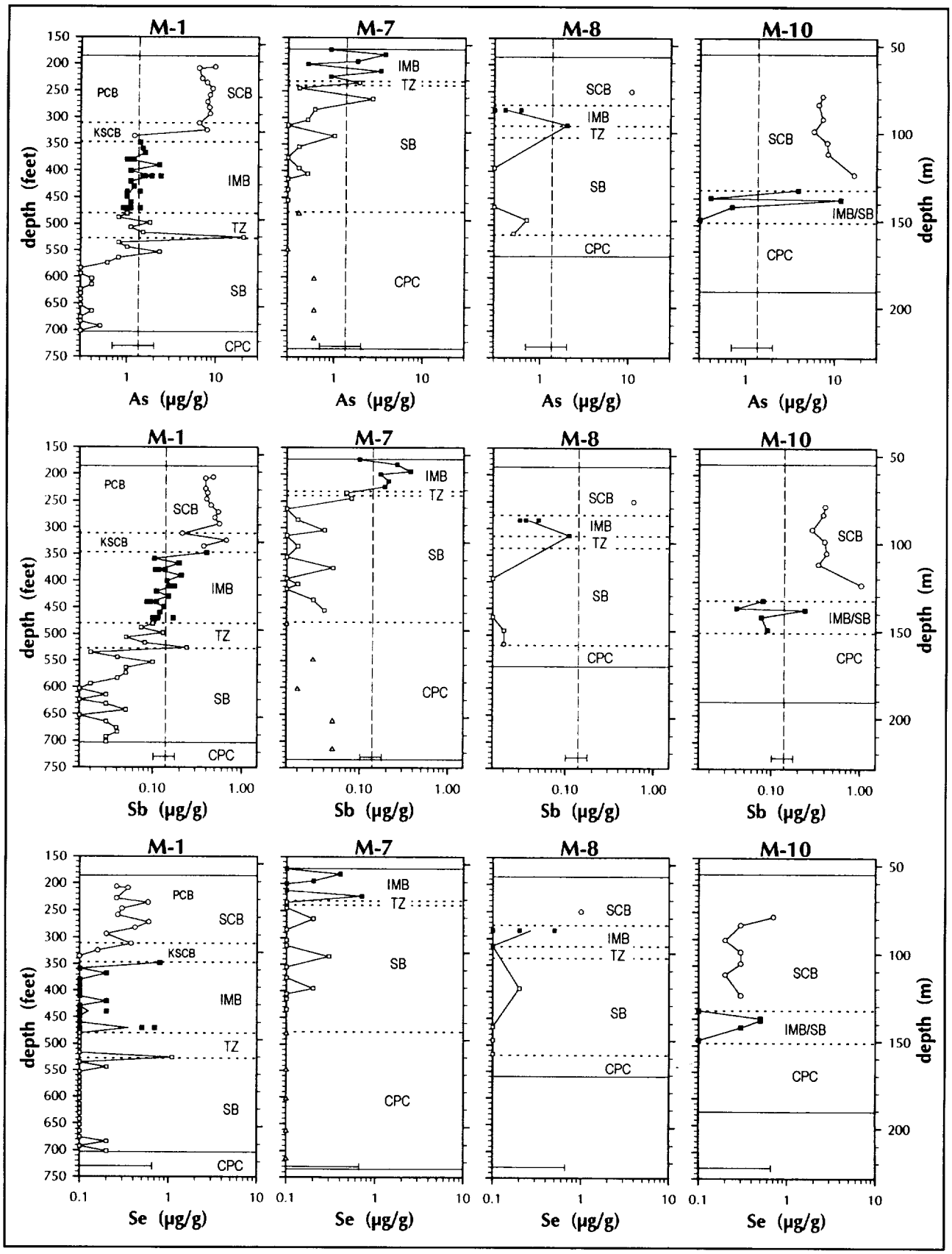
M-1
M-7
M-8
M-10
depth (feet)
depth (m)
PCB
SCB
KSCB
IMB
TZ
SB
CPC
IMB/SB
As (µg/g)
Sb (µg/g)
Se (µg/g)

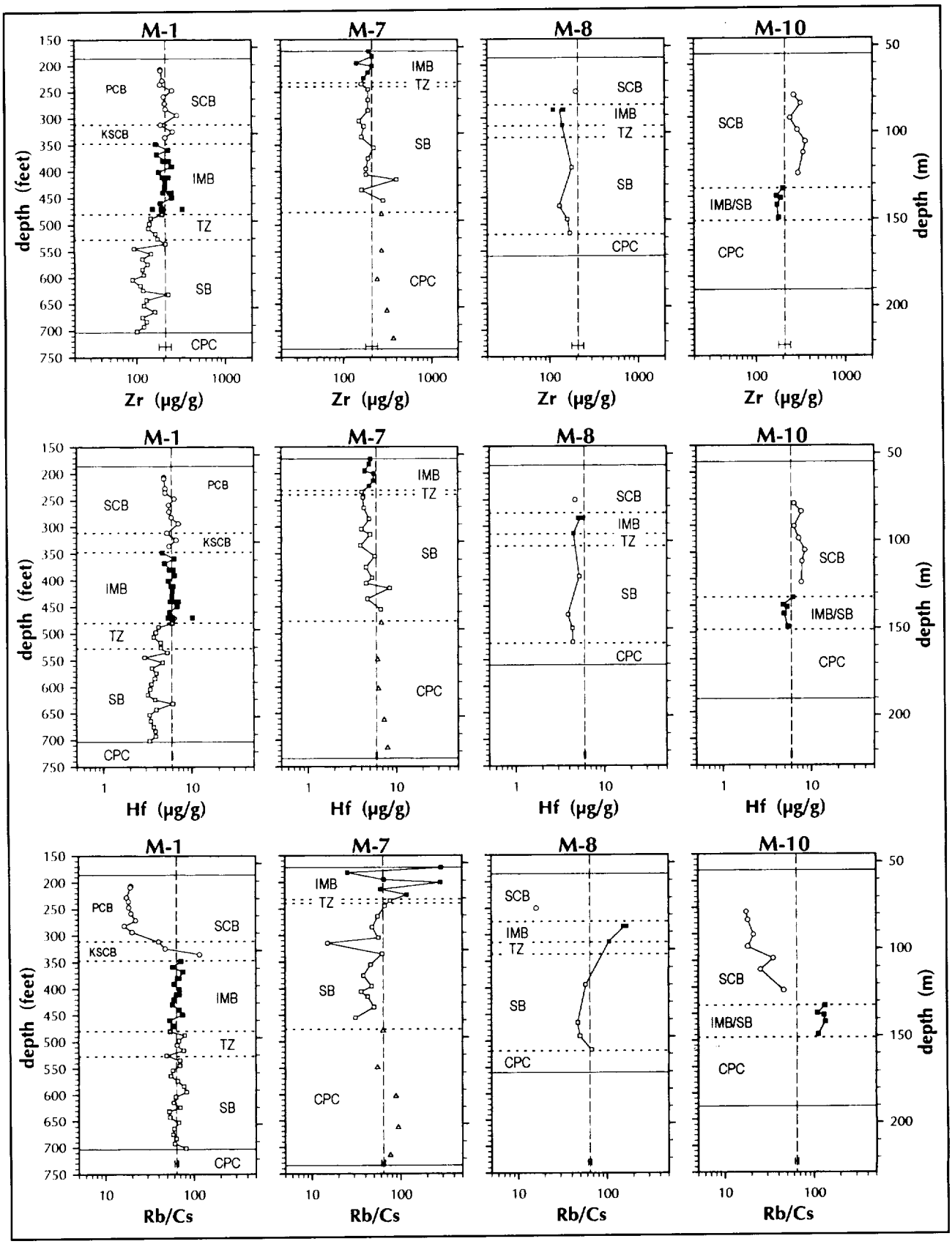
M-1
M-7
M-8
M-10
depth (feet)
depth (m)
PCB
KSCB
SCB
IMB
TZ
SB
IMB/SB
CPC
Zr (µg/g)
Hf (µg/g)
Rb/Cs
100
1000
1
10
150
200
250
300
350
400
450
500
550
600
650
700
750
50
100
150
200

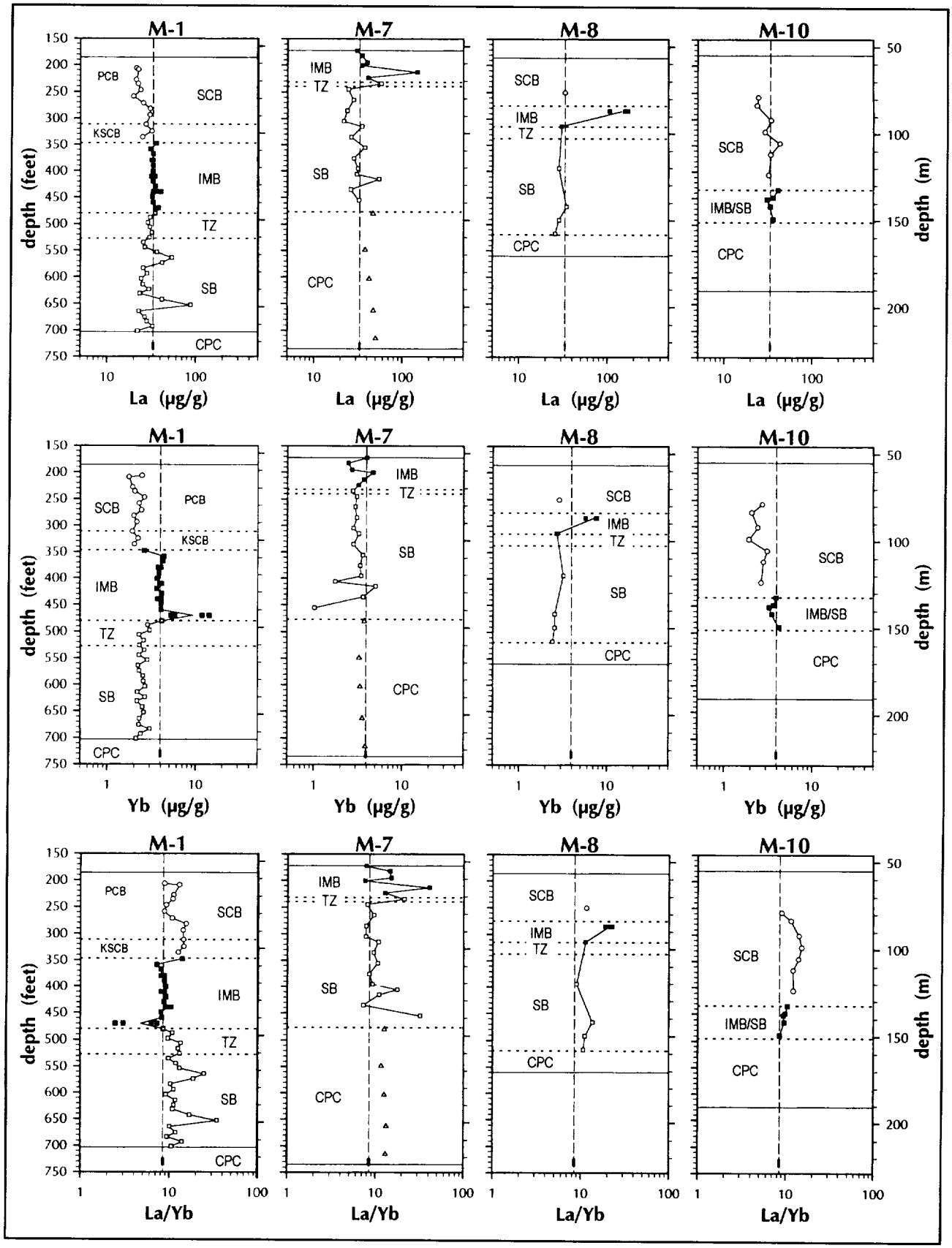
M-1
M-7
M-8
M-10
depth (feet)
depth (m)
PCB
KSCB
SCB
IMB
TZ
SB
CPC
IMB/SB
La (µg/g)
Yb (µg/g)
La/Yb

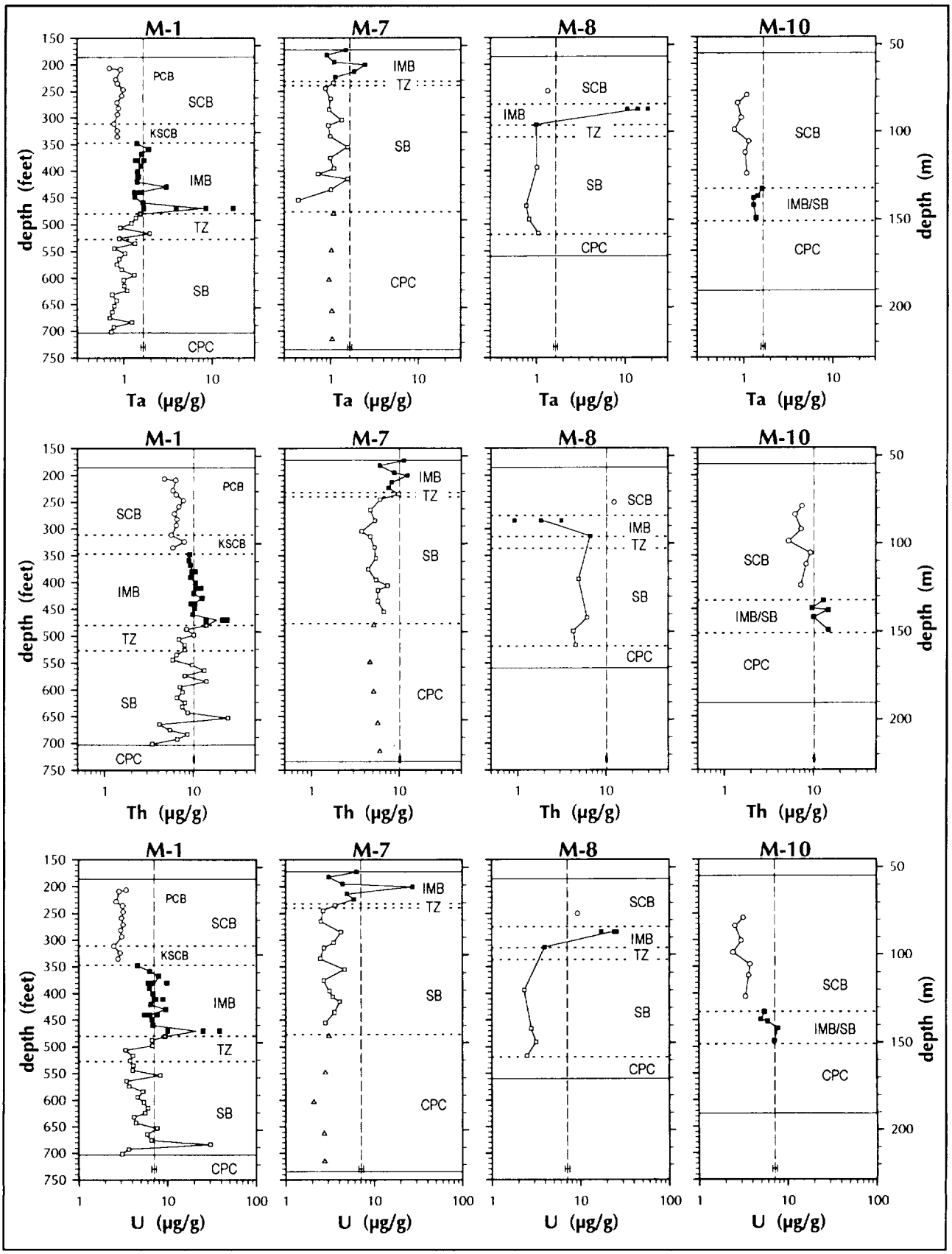
M-1
M-7
M-8
M-10
depth (feet)
depth (m)
PCB
SCB
KSCB
IMB
TZ
SB
CPC
IMB/SB
Ta (µg/g)
Th (µg/g)
U (µg/g)

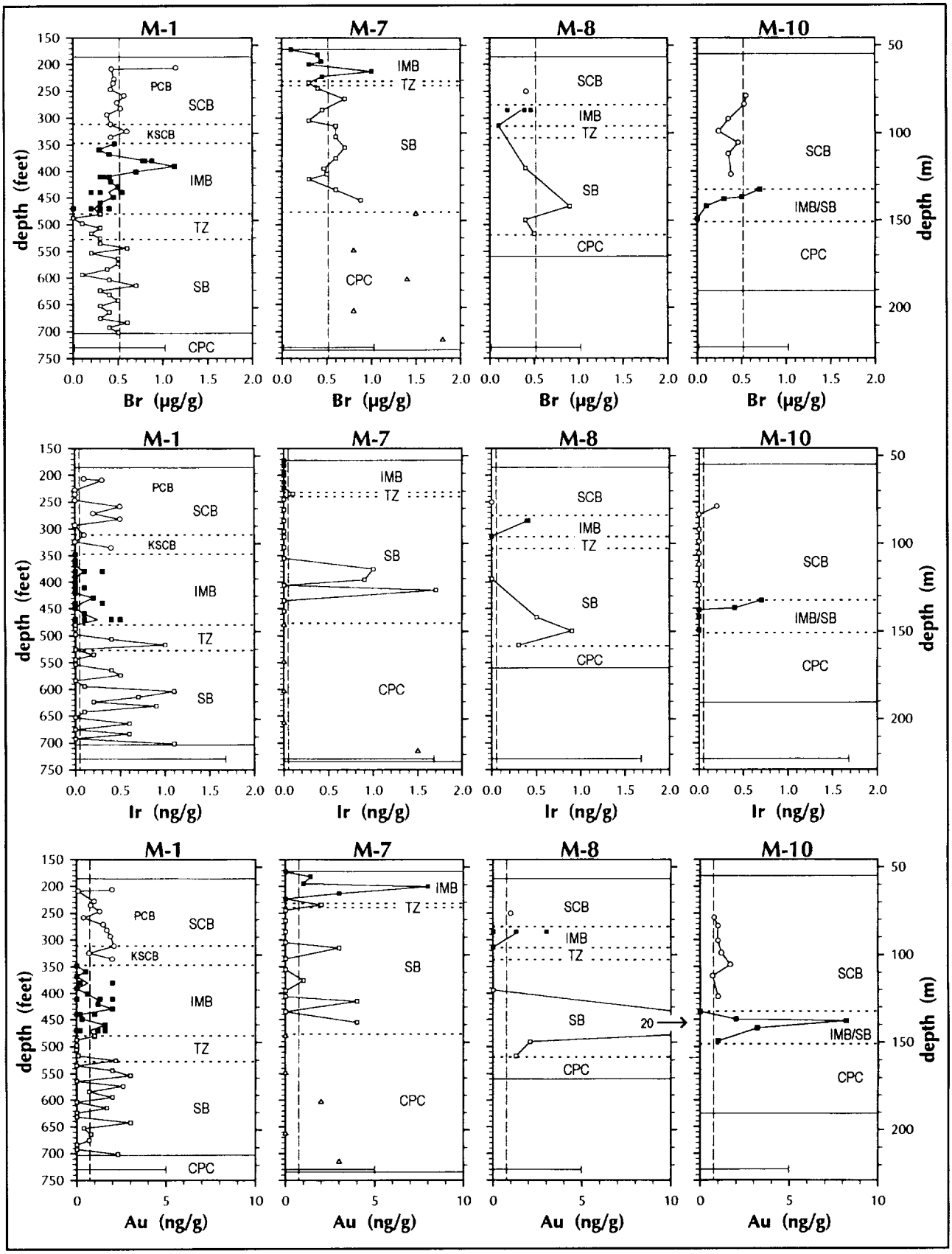
M-1
M-7
M-8
M-10
depth (feet)
depth (m)
PCB
SCB
KSCB
IMB
TZ
SB
CPC
IMB/SB
Br (µg/g)
Ir (ng/g)
Au (ng/g)
20

TABLE A1.1. RESULTS OF INSTRUMENTAL NEUTRON ACTIVATION ANALYSIS FOR BRECCIA SAMPLES FROM MANSON CORES
(page 1)

Sample*	Lab. Id.	Depth (m)	Unit	Fe_2O_3 (%)	CaO (%)	Na_2O (%)	K_2O (%)	Sc (μg/g)	Cr (μg/g)	Co (μg/g)	Ni (μg/g)	Zn (μg/g)	As (μg/g)
M-1 206.45	283.028	62.9	SCB	2.77	26.5	0.060	1.1	5.31	43.2	9.9	20	51	9.8
M-1 208.75	283.036	63.6	SCB	2.80	10.2	0.082	1.3	6.51	45.0	16.4	33	83	6.5
M-1 227.95	283.005	69.5	SCB	2.92	11.9	0.104	1.2	6.25	40.8	8.3	22	55	7.0
M-1 235.6	283.035	71.8	SCB	3.18	11.7	0.099	1.5	6.81	45.1	8.9	22	52	7.9
M-1 246.75	283.033	75.2	SCB	3.40	10.9	0.150	2.1	8.44	52.6	14.4	31	73	9.2
M-1 258.75	283.017	78.9	SCB	4.93	6.0	0.542	1.5	7.79	45.6	10.9	19	52	8.6
M-1 271.7	283.011	82.8	SCB	10.41	10.1	0.091	0.2	8.61	42.8	9.7	17	82	8.0
M-1 282.15	283.041	86.0	SCB	4.16	7.7	0.384	1.0	6.82	44.3	10.2	17	47	8.4
M-1 293.6	283.013	89.5	SCB	3.47	11.0	0.674	1.1	7.00	43.4	11.1	14	40	8.6
M-1 311.55	283.027	95.0	SCB	3.02	15.8	0.934	0.6	6.02	39.5	7.3	23	31	6.5
M-1 324.45	283.032	98.9	SCB	4.59	9.3	0.904	0.9	6.82	44.3	12.4	20	37	7.9
M-1 335.5	283.030	102.3	SCB	5.03	2.8	0.988	0.5	6.30	44.2	10.2	10	18	1.2
M-1 347.7	283.040	106.0	IMB	4.90	2.4	3.19	1.4	11.69	64.9	17.8	41	27	1.4
M-1 358.7	283.120	109.3	IMB	5.16	2.3	2.70	3.3	12.91	63.3	15.9	18	73	1.5
M-1 367.65	283.002	112.1	IMB	6.01	3.5	3.02	2.8	13.37	75.1	17.1	45	81	1.6
M-1 380.05A	283.101	115.8	IMB	5.65	2.4	3.01	3.1	12.52	50.5	14.8	22	53	1.0
M1- 380.05B	283.102	115.8	IMB	5.49	2.7	3.10	3.3	12.50	49.5	14.4	23	46	1.2
M-1 380.05C	283.103	115.8	IMB	5.53	2.6	2.99	3.3	12.10	49.3	14.7	16	52	1.1
M-1 380.05D	283.104	115.8	IMB	5.58	2.6	3.06	3.6	12.59	50.2	15.0	16	51	1.1
M-1 390.2	283.006	118.9	IMB	5.40	2.2	2.98	3.7	12.11	52.6	13.1	17	52	2.3
M-1 400.65	283.001	122.1	IMB	5.61	3.0	3.11	3.4	12.20	59.6	15.1	24	58	1.1
M-1 410.5A	283.105	125.1	IMB	5.68	3.0	3.41	3.1	12.96	52.8	15.0	19	59	1.5
M-1 410.5B	283.106	125.1	IMB	6.01	3.0	3.56	3.1	13.41	56.5	15.4	38	66	1.9
M-1 410.5C	283.107	125.1	IMB	5.67	3.0	3.53	2.8	13.07	54.5	14.5	15	64	1.6
M-1 410.5D	283.108	125.1	IMB	5.79	2.9	3.45	3.3	13.04	55.2	15.6	24	64	2.4
M-1 420.25	283.014	128.1	IMB	5.60	3.2	3.40	3.4	13.12	61.2	15.4	22	63	1.1
M-1 429.45	283.020	130.9	IMB	5.60	2.8	3.09	3.1	12.49	52.3	15.9	37	64	1.2
M-1 439.45A	283.109	133.9	IMB	6.08	3.7	3.54	3.1	13.67	59.3	15.7	16	64	1.0
M-1 439.45B	283.110	133.9	IMB	6.07	2.9	3.48	3.3	13.27	59.6	14.9	30	63	1.4
M-1 439.45C	283.111	133.9	IMB	5.59	2.7	3.31	3.1	12.76	54.1	14.8	16	57	1.0
M-1 439.45D	283.112	133.9	IMB	5.90	3.4	3.39	3.6	13.37	56.7	15.2	39	64	1.0
M-1 448.7	283.024	136.8	IMB	5.49	2.4	3.17	3.5	12.39	55.4	15.8	25	89	1.0
M-1 459.25	283.016	140.0	IMB	6.01	4.3	3.36	2.6	13.47	56.5	17.4	20	79	1.1
M-1 470.0A	283.113	143.3	IMB	5.91	3.7	3.24	3.1	12.84	55.2	16.4	18	77	0.9
M-1 470.0B	283.114	143.3	IMB	5.62	3.9	3.26	2.9	12.38	53.2	15.6	63	74	1.0
M-1 470.0C	283.115	143.3	IMB	6.19	3.8	3.25	2.6	13.08	56.7	17.3	19	80	1.1
M-1 470.0D	283.116	143.3	IMB	6.01	3.6	3.24	2.9	12.47	52.8	16.6	19	83	1.4
M-1 480.2	283.012	146.4	IMB	6.67	4.5	3.62	2.2	14.80	66.3	19.2	27	94	1.0
M-1 487.7	283.029	148.7	TZ	6.99	2.4	3.88	2.7	12.73	59.5	12.0	27	33	0.8
M-1 497.75	283.026	151.7	TZ	7.81	2.9	3.90	2.3	14.83	75.5	21.0	31	42	1.8
M-1 506.05	283.018	154.2	TZ	7.91	3.7	4.28	2.0	16.5	96.2	19.2	46	34	1.1
M-1 516.75	283.021	157.5	TZ	7.27	3.4	4.18	2.2	16.2	94.5	18.9	44	62	1.5
M-1 525.65	283.007	160.2	TZ	6.85	4.0	4.69	1.9	15.26	98.6	21.9	46	62	20.4
M-1 535.15	283.019	163.1	SB	5.99	4.0	4.58	2.0	14.70	88.2	19.5	36	76	0.8
M-1 544.0	283.023	165.8	SB	6.22	4.8	4.49	2.9	15.86	92.3	24.1	33	87	1.0
M-1 553.5	283.031	168.7	SB	8.92	4.5	4.63	1.6	17.4	116.0	24.3	38	82	2.3
M-1 564.0	283.009	171.9	SB	5.36	4.6	4.89	2.1	14.14	79.8	19.7	35	76	0.8
M-1 573.65	283.015	174.8	SB	6.75	4.3	4.69	1.8	16.7	99.2	22.3	45	82	0.6
M-1 583.8	283.037	177.9	SB	6.20	4.3	4.50	2.5	14.43	81.6	20.6	23	72	0.3
M-1 594.07	283.038	181.1	SB	6.59	4.7	4.60	2.2	15.36	82.8	20.1	45	76	0.3
M-1 603.67	283.039	184.0	SB	10.08	4.3	4.54	1.7	20.5	172.1	32.4	85	121	0.4
M-1 614.45	283.040	187.3	SB	6.02	5.2	4.45	2.1	15.47	116.2	19.6	42	65	0.4
M-1 623.55	283.041	190.1	SB	6.38	4.8	4.63	2.2	15.39	86.8	20.8	30	83	0.2
M-1 631.4	283.042	192.5	SB	6.67	4.7	4.48	1.6	15.57	91.0	22.1	48	76	0.1
M-1 642.42	283.043	195.8	SB	7.88	5.0	4.52	1.9	17.4	91.1	24.7	41	85	0.1
M-1 652.62	283.044	198.9	SB	7.31	9.7	4.14	1.7	17.4	103.6	22.8	35	86	0.1
M-1 664.35	283.045	202.5	SB	7.40	7.9	4.51	1.5	19.2	158.9	23.8	70	93	0.4
M-1 675.25	283.046	205.8	SB	7.67	9.5	4.03	1.5	19.9	130.6	25.3	53	95	0.3

TABLE A1.1. RESULTS OF INSTRUMENTAL NEUTRON ACTIVATION ANALYSIS FOR BRECCIA SAMPLES FROM MANSON CORES
(page 2)

Sample*	Lab. Id.	Se (μg/g)	Br (μg/g)	Rb (μg/g)	Sr (μg/g)	Zr (μg/g)	Sb (μg/g)	Cs (μg/g)	Ba (μg/g)	La (μg/g)	Ce (μg/g)	Nd (μg/g)	Sm (μg/g)
M-1 206.45	283.028	0.3	1.2	41	422	186	0.48	2.11	84	21.6	49.2	27	6.45
M-1 208.75	283.036	0.4	0.4	48	169	186	0.39	2.50	105	22.7	48.4	21	4.63
M-1 227.95	283.005	0.3	0.5	52	218	195	0.39	2.98	158	21.4	44.9	21	4.55
M-1 235.6	283.035	0.6	0.5	59	228	184	0.41	3.23	183	22.4	50.5	22	5.13
M-1 246.75	283.033	0.3	0.4	80	185	251	0.40	4.33	254	24.1	51.6	23	5.28
M-1 258.75	283.017	0.3	0.6	56	153	202	0.45	2.83	182	20.0	43.3	19	4.38
M-1 271.7	283.011	0.6	0.5	9	202	207	0.55	0.42	44	25.8	53.9	23	5.15
M-1 282.15	283.041	0.4	0.5	44	125	212	0.50	2.66	119	30.8	63.3	29	5.21
M-1 293.6	283.013	0.2	0.4	43	189	284	0.56	2.15	154	30.6	63.1	28	5.38
M-1 311.55	283.027	0.4	0.4	19	204	187	0.21	0.48	104	27.5	54.6	23	4.60
M-1 324.45	283.032	0.2	0.6	26	125	254	0.67	0.54	168	32.1	65.8	31	5.51
M-1 335.5	283.030	0.0	0.4	15	188	210	0.37	0.13	133	25.1	51.7	22	4.52
M-1 347.7	283.040	0.8	0.5	51	246	163	0.40	0.71	313	36.0	73.5	31	6.13
M-1 358.7	283.120	0.0	0.3	114	214	225	0.10	1.97	689	30.9	65.4	30	6.72
M-1 367.65	283.002	0.2	0.4	114	244	168	0.20	1.51	659	33.3	65.9	28	6.10
M-1 380.05A	283.101	0.1	0.8	120	209	198	0.11	1.76	636	32.0	67.0	29	6.35
M1- 380.05B	283.102	0.0	0.8	119	212	230	0.11	1.77	649	32.6	67.3	31	6.39
M-1 380.05C	283.103	0.0	0.9	118	209	230	0.12	1.80	626	31.9	66.2	29	6.27
M-1 380.05D	283.104	0.0	0.8	119	203	222	0.14	1.75	637	32.0	67.0	31	6.38
M-1 390.2	283.006	0.0	1.1	126	203	247	0.21	2.11	656	32.9	68.6	31	6.49
M-1 400.65	283.001	0.0	0.7	132	225	178	0.14	1.92	667	32.9	66.5	28	6.16
M-1 410.5A	283.105	0.0	0.3	121	228	197	0.15	1.89	668	31.7	66.1	31	6.33
M-1 410.5B	283.106	0.1	0.3	119	245	228	0.16	1.73	694	33.7	70.7	32	6.80
M-1 410.5C	283.107	0.0	0.4	126	241	196	0.17	1.84	701	32.7	67.9	31	6.71
M-1 410.5D	283.108	0.0	0.4	125	248	205	0.18	1.91	688	34.6	71.7	33	6.71
M-1 420.25	283.014	0.2	0.4	119	259	209	0.11	2.01	656	33.0	67.7	30	6.35
M-1 429.45	283.020	0.0	0.5	116	258	208	0.15	2.02	631	35.0	70.7	32	6.62
M-1 439.45A	283.109	0.2	0.3	114	244	199	0.09	1.67	719	37.5	75.6	33	6.72
M-1 439.45B	283.110	0.0	0.6	119	237	235	0.09	1.76	698	33.1	68.4	30	6.31
M-1 439.45C	283.111	0.0	0.5	120	231	199	0.09	1.74	694	37.8	75.7	33	6.58
M-1 439.45D	283.112	0.0	0.2	121	236	246	0.11	1.77	735	40.4	80.2	33	6.82
M-1 448.7	283.024	0.0	0.5	130	232	248	0.13	1.74	667	32.4	67.3	29	6.57
M-1 459.25	283.016	0.1	0.3	100	278	186	0.12	1.87	613	33.0	67.9	30	6.78
M-1 470.0A	283.113	0.0	0.4	111	267	197	0.10	1.89	649	36.0	71.5	32	7.45
M-1 470.0B	283.114	0.5	0.3	108	278	190	0.10	1.79	647	35.5	71.8	32	9.70
M-1 470.0C	283.115	0.1	0.0	111	269	326	0.11	1.86	663	37.7	75.0	34	7.04
M-1 470.0D	283.116	0.7	0.2	107	258	152	0.17	1.79	645	34.9	71.8	33	11.24
M-1 480.2	283.012	0.0	0.3	95	294	194	0.10	1.76	670	34.8	71.3	32	6.99
M-1 487.7	283.029	0.0	0.0	87	197	145	0.07	1.09	659	30.6	62.0	27	5.78
M-1 497.75	283.026	0.0	0.1	79	228	140	0.13	1.16	660	28.7	59.9	27	5.78
M-1 506.05	283.018	0.0	0.3	67	285	136	0.05	1.03	682	30.4	60.9	25	5.40
M-1 516.75	283.021	0.0	0.2	74	295	163	0.08	0.96	708	31.9	62.0	28	5.71
M-1 525.65	283.007	1.1	0.3	69	329	172	0.24	1.41	751	30.0	62.3	30	5.92
M-1 535.15	283.019	0.1	0.3	72	367	210	0.02	1.03	778	25.5	53.6	25	5.47
M-1 544.0	283.023	0.2	0.6	73	416	94	0.04	1.05	759	26.6	54.4	26	5.06
M-1 553.5	283.031	0.0	0.2	54	370	146	0.10	0.93	747	36.6	73.3	34	7.40
M-1 564.0	283.009	0.0	0.5	61	409	116	0.05	1.11	814	53.9	101	39	6.96
M-1 573.65	283.015	0.0	0.5	61	348	133	0.05	0.92	673	42.0	78.5	32	5.99
M-1 583.8	283.037	0.0	0.4	69	370	116	0.04	0.89	723	25.6	53.4	23	5.28
M-1 594.07	283.038	0.1	0.1	64	380	120	0.02	0.77	761	28.4	56.5	25	5.10
M-1 603.67	283.039	0.0	0.4	52	300	90	0.00	0.83	557	24.2	50.6	22	4.91
M-1 614.45	283.040	0.0	0.7	63	412	110	0.03	1.06	715	25.4	51.5	23	4.80
M-1 623.55	283.041	0.0	0.3	71	396	118	0.01	1.01	769	29.8	62.5	32	6.05
M-1 631.4	283.042	0.0	0.4	54	385	225	0.03	1.02	853	23.5	48.9	22	4.82
M-1 642.42	283.043	0.0	0.5	62	419	129	0.05	1.15	784	41.9	84.1	36	6.91
M-1 652.62	283.044	0.0	0.3	51	380	120	0.01	0.75	610	88.2	170	61	9.32
M-1 664.35	283.045	0.0	0.4	53	350	160	0.03	0.88	570	22.9	46.9	24	5.09
M-1 675.25	283.046	0.0	0.3	53	366	116	0.04	0.90	665	26.7	54.1	25	5.29

TABLE A1.1. RESULTS OF INSTRUMENTAL NEUTRON ACTIVATION ANALYSIS FOR BRECCIA SAMPLES FROM MANSON CORES
(page 3)

Sample*	Lab. Id.	Eu (μg/g)	Tb (μg/g)	Yb (μg/g)	La (μg/g)	Hf (μg/g)	Ta (μg/g)	W (μg/g)	Ir (μg/g)	Au (μg/g)	Th (μg/g)	U (μg/g)	Mass (mg)
M-1 206.45	283.028	1.45	0.91	2.46	0.355	4.87	0.70	0.6	0.1	2.0	4.76	3.5	123
M-1 208.75	283.036	0.92	0.59	1.76	0.263	4.87	0.93	0.7	0.3	0.1	6.38	2.9	134
M-1 227.95	283.005	1.02	0.61	1.93	0.286	5.03	0.82	0.7	0.0	1.0	5.95	2.7	139
M-1 235.6	283.035	1.18	0.68	2.05	0.302	5.01	0.86	0.7	0.0	0.8	6.49	3.2	157
M-1 246.75	283.033	1.11	0.80	2.63	0.384	6.35	0.99	0.8	0.0	1.3	7.79	3.2	128
M-1 258.75	283.017	0.89	0.63	2.29	0.341	5.50	0.96	0.9	0.5	0.4	6.93	3.1	165
M-1 271.7	283.011	1.05	0.78	2.42	0.340	5.54	0.85	0.7	0.2	1.5	6.18	3.2	188
M-1 282.15	283.041	0.98	0.59	2.00	0.294	5.88	0.88	0.8	0.5	1.7	6.59	3.0	160
M-1 293.6	283.013	1.17	0.69	2.15	0.320	7.08	0.86	1.0	0.0	1.9	6.49	3.1	161
M-1 311.55	283.027	1.17	0.63	1.92	0.286	5.26	0.78	0.6	0.1	2.1	5.71	2.5	137
M-1 324.45	283.032	1.08	0.72	2.22	0.335	6.67	0.85	0.8	0.0	0.7	7.98	3.0	158
M-1 335.5	283.030	0.91	0.62	2.01	0.294	5.55	0.85	0.8	0.4	2.0	5.91	2.8	151
M-1 347.7	283.040	1.16	0.80	2.59	0.385	4.63	1.40	0.7	0.0	0.0	9.10	4.6	163
M-1 358.7	283.120	1.36	1.15	4.30	0.615	6.30	1.89	1.4	0.0	0.5	8.91	6.3	175
M-1 367.65	283.002	1.29	1.03	4.20	0.610	4.88	1.58	0.7	0.0	0.0	9.28	8.0	205
M-1 380.05A	283.101	1.26	1.05	3.97	0.590	5.57	1.43	1.1	0.0	2.0	9.75	6.0	177
M1- 380.05B	283.102	1.29	0.98	3.73	0.546	6.16	1.39	0.3	0.1	0.2	9.62	6.1	208
M-1 380.05C	283.103	1.27	1.01	3.89	0.563	6.01	1.69	0.6	0.3	0.2	9.81	6.8	185
M-1 380.05D	283.104	1.27	1.00	3.88	0.564	6.09	1.36	0.8	0.0	0.1	10.48	9.8	220
M-1 390.2	283.006	1.22	1.02	3.77	0.558	6.43	1.56	1.2	0.0	0.0	9.38	6.2	178
M-1 400.65	283.001	1.22	0.95	3.63	0.539	5.42	1.42	0.8	0.0	0.6	10.53	6.9	177
M-1 410.5A	283.105	1.38	1.01	3.90	0.582	5.80	1.43	0.9	0.0	1.3	12.2	7.3	165
M-1 410.5B	283.106	1.47	1.06	3.97	0.588	6.10	1.47	0.9	0.1	0.0	11.48	7.1	174
M-1 410.5C	283.107	1.41	1.06	4.05	0.588	5.90	1.43	0.5	0.0	2.0	10.95	8.8	166
M-1 410.5D	283.108	1.40	1.06	3.92	0.574	5.78	1.46	0.2	0.0	1.3	10.50	7.4	167
M-1 420.25	283.014	1.29	0.94	3.60	0.538	5.97	1.41	0.9	0.0	1.2	10.08	6.4	170
M-1 429.45	283.020	1.29	1.11	4.04	0.584	5.95	3.01	0.2	0.2	2.0	12.53	9.5	201
M-1 439.45A	283.109	1.31	1.04	4.01	0.617	5.66	1.50	0.1	0.3	0.0	10.19	6.3	200
M-1 439.45B	283.110	1.26	0.98	3.69	0.556	6.23	1.31	0.9	0.0	0.0	9.42	5.5	170
M-1 439.45C	283.111	1.24	1.00	3.66	0.543	5.68	1.43	0.6	0.0	0.2	10.00	6.2	202
M-1 439.45D	283.112	1.26	1.02	3.90	0.585	7.02	1.58	0.6	0.0	1.0	10.47	7.6	190
M-1 448.7	283.024	1.24	1.05	4.02	0.592	6.78	1.32	0.9	0.0	0.3	10.30	6.6	210
M-1 459.25	283.016	1.35	1.05	4.01	0.594	5.61	1.64	1.2	0.1	1.6	9.81	6.9	233
M-1 470.0A	283.113	1.39	1.45	5.74	0.810	5.36	3.87	0.8	0.4	1.6	14.0	10.0	189
M-1 470.0B	283.114	1.39	2.53	11.76	1.700	6.00	8.48	2.8	0.0	0.0	21.3	25.1	181
M-1 470.0C	283.115	1.43	1.17	5.18	0.783	10.20	1.67	0.7	0.1	1.2	14.1	10.0	188
M-1 470.0D	283.116	1.40	3.15	14.19	2.010	5.55	17.30	2.3	0.5	0.2	24.2	38.5	228
M-1 480.2	283.012	1.49	1.11	4.07	0.603	5.98	1.53	1.3	0.0	1.0	14.1	9.4	232
M-1 487.7	283.029	1.13	0.88	2.82	0.389	4.17	1.36	1.0	0.0	0.0	8.39	6.7	173
M-1 497.75	283.026	1.23	0.85	2.98	0.445	3.90	1.22	1.2	0.0	0.0	10.20	6.8	159
M-1 506.05	283.018	1.27	0.71	2.26	0.330	3.69	0.91	1.2	0.4	0.0	6.85	3.4	170
M-1 516.75	283.021	1.35	0.82	2.55	0.359	4.43	1.95	1.4	1.0	0.1	8.00	4.1	162
M-1 525.65	283.007	1.14	0.74	2.29	0.354	4.46	0.89	1.2	0.0	2.2	8.04	3.8	165
M-1 535.15	283.019	1.19	0.78	2.61	0.394	5.26	1.33	1.3	0.2	0.0	6.45	4.1	174
M-1 544.0	283.023	1.20	0.71	2.26	0.323	2.91	0.78	1.5	0.0	2.0	5.85	4.1	138
M-1 553.5	283.031	1.78	0.97	2.81	0.406	4.70	1.03	1.5	0.0	3.0	9.71	8.3	180
M-1 564.0	283.009	1.36	0.80	2.20	0.319	3.49	0.89	0.0	0.4	0.0	13.3	3.5	143
M-1 573.65	283.015	1.35	0.72	2.26	0.338	3.95	0.84	1.2	0.5	2.6	8.01	3.7	159
M-1 583.8	283.037	1.25	0.72	2.50	0.366	3.80	0.94	1.1	0.0	0.7	14.0	5.3	166
M-1 594.07	283.038	1.26	0.73	2.54	0.378	3.48	1.31	1.5	0.1	2.0	7.03	4.6	154
M-1 603.67	283.039	1.13	0.71	2.65	0.384	3.35	1.00	1.3	1.1	0.0	7.56	5.4	150
M-1 614.45	283.040	1.20	0.65	2.18	0.307	3.16	1.01	1.7	0.7	1.7	6.52	6.0	161
M-1 623.55	283.041	1.39	0.84	2.65	0.382	3.83	1.09	0.0	0.2	0.0	8.09	5.6	153
M-1 631.4	283.042	1.26	0.66	2.16	0.317	6.08	0.74	1.8	0.9	0.0	7.49	4.2	161
M-1 642.42	283.043	1.62	0.87	2.48	0.343	3.94	0.83	1.7	0.1	3.0	8.65	4.4	198
M-1 652.62	283.044	1.61	0.91	2.56	0.381	3.31	0.78	1.1	0.0	0.4	24.7	7.7	130
M-1 664.35	283.045	1.28	0.74	2.28	0.367	3.41	0.74	1.7	0.6	0.8	4.16	5.9	150
M-1 675.25	283.046	1.38	0.70	2.27	0.338	3.69	0.70	1.5	0.0	0.7	5.45	6.6	183

TABLE A1.1. RESULTS OF INSTRUMENTAL NEUTRON ACTIVATION ANALYSIS FOR BRECCIA SAMPLES FROM MANSON CORES
(page 4)

Sample*	Lab. Id.	Depth (m)	Unit	Fe_2O_3 (%)	CaO (%)	Na_2O (%)	K_2O (%)	Sc (μg/g)	Cr (μg/g)	Co (μg/g)	Ni (μg/g)	Zn (μg/g)	As (μg/g)
M-1 683.55	283.047	208.3	SB	7.33	4.8	4.30	1.9	17.0	89.7	25.3	60	89	0.0
M-1 692.5	283.048	211.1	SB	8.41	4.6	4.48	2.1	18.1	123.1	27.4	40	111	0.5
M-1 701.52	283.049	213.8	SB	7.09	4.5	4.73	2.5	16.8	80.4	22.9	30	82	0.3
M-7 172.6	293.001	52.6	IMB	4.63	2.1	2.94	3.9	13.38	56.0	12.1	22	82	0.9
M-7 182.0	295.001	55.5	IMB	3.28	2.1	3.36	2.1	9.93	49.0	13.1	24	92	3.7
M-7 194.9	295.002	59.4	IMB	5.19	1.6	2.95	2.1	10.43	48.1	15.4	16	147	1.8
M-7 200.18	293.002	61.0	IMB	5.72	3.3	3.41	3.9	14.90	57.3	21.9	23	108	0.5
M-7 213.0	295.003	64.9	IMB	5.73	1.5	4.07	1.7	16.2	81.0	12.7	50	34	3.3
M-7 223.45	293.003	68.1	IMB	5.16	1.8	3.59	2.8	11.74	63.9	12.4	43	44	0.9
M-7 234.78	293.004	71.6	TZ	6.15	3.4	3.88	2.1	13.71	62.4	17.7	50	53	1.9
M-7 245.0	293.005	74.7	SB	11.07	4.2	3.51	1.7	19.9	68.6	28.9	80	84	0.4
M-7 265.0	293.006	80.8	SB	10.55	5.0	3.66	1.7	20.8	83.4	39.3	50	86	2.7
M-7 285.1	293.007	86.9	SB	10.00	5.7	3.78	1.3	20.1	67.0	31.5	50	95	0.6
M-7 305.0	293.008	93.0	SB	10.18	5.4	3.56	1.9	20.3	79.9	33.3	45	107	0.5
M-7 315.0	293.009	96.0	SB	8.48	5.6	3.50	1.6	18.2	65.0	25.2	30	87	0.3
M-7 335.0	293.010	102.1	SB	10.58	4.8	3.50	1.7	20.3	74.1	32.3	50	98	1.0
M-7 355.03	293.011	108.2	SB	9.89	6.3	4.27	1.5	20.3	82.5	29.0	60	95	0.4
M-7 375.32	293.012	114.4	SB	8.88	6.3	3.79	2.0	18.4	91.7	26.8	40	88	0.0
M-7 395.37	293.013	120.5	SB	11.98	5.6	3.55	1.5	22.9	81.6	34.0	50	109	0.4
M-7 405.8	293.014	123.7	SB	6.19	4.0	4.64	2.4	11.59	68.9	16.8	40	73	0.5
M-7 415.18	293.015	126.5	SB	13.48	6.7	3.49	0.6	23.3	76.7	37.1	30	126	0.0
M-7 435.0	293.016	132.6	SB	7.00	4.8	4.88	2.0	16.5	73.1	20.3	19	84	0.0
M-7 455.0	293.017	138.7	SB	5.21	4.5	5.72	1.2	4.48	11.3	11.6	4	51	0.3
M-7 479.98	293.018	146.3	CPC	12.02	5.7	3.94	1.9	24.9	112.0	37.0	30	123	0.4
M-7 548.57	293.019	167.2	CPC	10.28	7.0	4.36	0.8	19.8	78.1	31.2	60	95	0.3
M-7 603.36	293.020	183.9	CPC	11.82	5.6	4.03	1.6	24.2	101.0	43.5	80	116	0.6
M-7 662.8	293.021	202.0	CPC	10.78	6.7	4.33	1.6	20.3	79.3	31.9	20	125	0.6
M-7 715.4	293.022	218.1	CPC	12.07	7.1	3.90	1.8	25.2	89.4	41.9	70	128	0.6
M-8 250.6	293.034	76.4	SCB	3.97	8.2	0.354	2.2	10.08	57.3	15.7	24	77	10.8
M-8 285.3A	293.035	87.0	IMB	4.48	6.7	3.38	4.6	2.05	0.5	5.5	3	204	0.6
M-8 285.3B	295.010	87.0	IMB	3.47	7.3	3.15	5.5	1.51	1.3	4.3	0	145	0.4
M-8 285.3C	295.011	87.0	IMB	4.71	7.0	3.68	3.5	2.21	1.8	5.5	9	84	0.1
M-8 313.9	293.036	95.7	IMB	3.93	3.7	3.91	2.1	12.20	64.0	12.2	16	64	2.0
M-8 393.7	293.037	120.0	SB	12.77	4.5	3.22	1.2	23.4	67.3	42.4	90	157	0.0
M-8 465.8	293.038	142.0	SB	7.83	5.3	4.02	1.1	18.1	77.1	25.1	50	83	0.0
M-8 491.1	293.039	149.7	SB	8.97	5.9	4.15	1.6	19.7	80.9	28.4	40	101	0.7
M-8 517.1	293.040	157.6	SB	10.09	3.5	3.85	1.8	18.9	71.4	34.7	60	142	0.5
M-10 258.6	293.023	78.8	SCB	4.18	6.7	0.457	1.1	7.97	50.8	11.7	15	63	7.2
M-10 274.2	293.024	83.6	SCB	2.96	6.7	0.280	1.1	6.54	42.7	8.0	21	28	6.6
M-10 301.8	293.025	92.0	SCB	4.78	3.8	0.644	0.8	8.10	47.0	13.0	35	42	7.3
M-10 324.2	293.026	98.8	SCB	2.28	7.7	0.490	0.7	5.23	37.1	7.3	13	23	5.8
M-10 346.1	293.027	105.5	SCB	3.24	1.7	1.90	0.6	11.40	58.5	13.4	35	29	8.2
M-10 366.8	293.028	111.8	SCB	5.19	0.8	1.36	0.3	8.55	52.8	12.7	32	39	8.4
M-10 405.9	293.029	123.7	SCB	3.71	3.5	1.76	0.5	8.38	52.0	11.0	30	740	16.6
M-10 434.4	293.030	132.4	IMB/SB	6.49	3.3	3.97	3.8	16.3	76.3	15.2	30	79	3.9
M-10 448.9	293.031	136.8	IMB/SB	8.28	3.8	4.20	1.9	15.60	68.9	21.7	40	95	0.4
M-10 452.4	293.032	137.9	IMB/SB	7.00	2.9	3.68	2.3	13.89	66.1	18.8	25	82	11.8
M-10 465.6	293.033	141.9	IMB/SB	7.30	2.8	3.80	2.8	12.56	62.1	18.1	22	85	0.7
M-10 489.5	295.012	149.2	IMB/SB	7.67	3.2	4.89	2.0	16.9	83.8	20.6	30	137	0.2
σ†				0.06	0.3	0.03	0.5	0.13	0.6	0.2	12	5	0.4

TABLE A1.1. RESULTS OF INSTRUMENTAL NEUTRON ACTIVATION ANALYSIS FOR BRECCIA SAMPLES FROM MANSON CORES
(page 5)

Sample*	Lab. Id.	Se (μg/g)	Br (μg/g)	Rb (μg/g)	Sr (μg/g)	Zr (μg/g)	Sb (μg/g)	Cs (μg/g)	Ba (μg/g)	La (μg/g)	Ce (μg/g)	Nd (μg/g)	Sm (μg/g)
M-1 683.55	283.047	0.2	0.6	63	390	130	0.04	0.99	710	28.0	57.2	24	5.44
M-1 692.5	283.048	0.0	0.4	58	380	120	0.03	0.95	750	32.8	69.1	33	6.26
M-1 701.52	283.049	0.2	0.5	97	480	100	0.03	1.19	880	22.1	45.7	20	4.78
M-7 172.6	293.001	0.1	0.1	135	239	193	0.10	0.47	838	30.9	73.3	33	7.49
M-7 182.0	295.001	0.4	0.4	84	250	210	0.26	3.31	575	35.5	66.9	27	5.51
M-7 194.9	295.002	0.2	0.4	90	220	140	0.37	1.38	579	40.3	76.4	32	6.48
M-7 200.18	293.002	0.0	0.3	141	230	210	0.17	0.50	920	35.0	82.6	38	8.58
M-7 213.0	295.003	0.0	1.0	60	240	190	0.21	1.00	460	148.5	258	88	15.87
M-7 223.45	293.003	0.7	0.5	102	260	170	0.19	0.86	707	41.0	78.2	32	7.26
M-7 234.78	293.004	0.0	0.3	79	330	160	0.07	1.03	661	57.8	99.7	34	6.60
M-7 245.0	293.005	0.0	0.4	60	240	190	0.08	0.90	538	24.6	51.2	25	5.89
M-7 265.0	293.006	0.2	0.7	63	300	190	0.01	1.14	622	28.1	58.0	26	6.01
M-7 285.1	293.007	0.0	0.5	53	290	190	0.02	1.10	538	23.8	51.2	29	6.16
M-7 305.0	293.008	0.0	0.3	66	310	150	0.04	1.17	664	21.7	46.4	23	5.49
M-7 315.0	293.009	0.1	0.6	48	370	170	0.01	3.19	560	34.9	73.9	36	7.88
M-7 335.0	293.010	0.3	0.6	64	300	160	0.02	1.03	650	26.5	54.8	25	5.94
M-7 355.03	293.011	0.0	0.7	45	310	220	0.00	0.98	550	37.8	80.2	40	8.52
M-7 375.32	293.012	0.0	0.6	65	440	190	0.05	1.70	660	28.3	60.2	30	6.55
M-7 395.37	293.013	0.2	0.5	62	300	180	0.01	1.31	620	31.7	67.8	32	7.62
M-7 405.8	293.014	0.0	0.5	77	430	180	0.02	2.15	1,190	30.6	61.9	26	4.91
M-7 415.18	293.015	0.1	0.3	47	330	400	0.00	1.10	680	54.8	120.5	64	13.95
M-7 435.0	293.016	0.0	0.6	75	370	160	0.03	1.49	740	26.2	53.7	24	5.46
M-7 455.0	293.017	0.1	0.9	47	544	281	0.04	1.52	933	32.4	57.3	20	3.12
M-7 479.98	293.018	0.0	1.5	38	400	270	0.00	0.60	650	47.1	100.9	51	10.75
M-7 548.57	293.019	0.0	0.8	45	370	270	0.03	0.82	730	38.4	81.6	40	8.92
M-7 603.36	293.020	0.0	1.4	53	320	240	0.02	0.60	800	42.5	88.9	47	9.20
M-7 662.8	293.021	0.1	0.8	46	400	310	0.05	0.49	760	47.3	100.3	48	10.38
M-7 715.4	293.022	0.0	1.8	36	420	370	0.05	0.47	640	50.3	105.6	51	10.85
M-8 250.6	293.034	1.0	0.4	91	203	200	0.59	5.66	192	33.3	66.1	28	6.40
M-8 285.3A	293.035	0.0	0.5	117	406	141	0.05	0.77	1,760	158	209	71	13.26
M-8 285.3B	295.010	0.5	0.4	146	355	145	0.04	0.88	2,340	107	137	51	8.82
M-8 285.3C	295.011	0.2	0.2	96	373	110	0.03	0.62	1,340	171	214	73	13.06
M-8 313.9	293.036	0.0	0.1	79	310	140	0.11	0.75	713	30.4	61.0	26	5.55
M-8 393.7	293.037	0.2	0.4	45	250	180	0.00	0.78	530	28.4	60.4	30	6.84
M-8 465.8	293.038	0.0	0.9	49	320	130	0.01	1.05	678	34.5	68.6	31	6.16
M-8 491.1	293.039	0.0	0.4	53	310	160	0.02	1.07	573	28.3	58.0	28	5.96
M-8 517.1	293.040	0.0	0.5	71	290	170	0.02	1.06	720	25.6	54.0	26	5.69
M-10 258.6	293.023	0.7	0.6	57	135	265	0.40	3.27	170	24.3	52.6	24	5.38
M-10 274.2	293.024	0.3	0.5	51	138	316	0.39	2.82	175	23.6	51.3	23	4.64
M-10 301.8	293.025	0.2	0.4	44	132	242	0.29	2.09	150	34.0	71.3	30	5.93
M-10 324.2	293.026	0.3	0.2	32	105	292	0.40	1.77	103	29.0	61.1	26	5.12
M-10 346.1	293.027	0.3	0.5	24	140	360	0.42	0.70	105	42.9	81.7	34	6.19
M-10 366.8	293.028	0.2	0.4	8	108	340	0.34	0.31	58	33.8	71.0	29	6.51
M-10 405.9	293.029	0.3	0.4	17	204	298	1.03	0.37	128	32.0	66.6	27	5.85
M-10 434.4	293.030	0.1	0.7	109	260	200	0.08	0.82	1,180	40.6	83.3	37	7.73
M-10 448.9	293.031	0.5	0.5	71	280	170	0.04	0.65	579	35.6	73.7	33	7.40
M-10 452.4	293.032	0.5	0.3	101	240	190	0.24	0.78	634	30.5	64.9	30	6.61
M-10 465.6	293.033	0.3	0.1	92	221	172	0.08	0.69	596	33.1	70.1	32	7.05
M-10 489.5	295.012	0.0	0.0	72	280	180	0.09	0.65	520	35.7	74.7	27	7.42
σ†		0.3	0.3	2	14	16	0.02	0.03	12	0.4	0.7	2	0.07

TABLE A1.1. RESULTS OF INSTRUMENTAL NEUTRON ACTIVATION ANALYSIS FOR BRECCIA SAMPLES FROM MANSON CORES
(page 6)

Sample*	Lab. Id.	Eu (μg/g)	Tb (μg/g)	Yb (μg/g)	La (μg/g)	Hf (μg/g)	Ta (μg/g)	W (μg/g)	Ir (μg/g)	Au (μg/g)	Th (μg/g)	U (μg/g)	Mass (mg)
M-1 683.55	283.047	1.30	0.90	2.98	0.432	3.86	1.23	2.2	0.6	0.0	8.60	30.4	185
M-1 692.5	283.048	1.46	0.83	2.36	0.344	3.89	0.77	1.3	0.0	0.0	6.60	3.7	166
M-1 701.52	283.049	1.26	0.70	2.09	0.294	3.29	0.72	1.6	1.1	2.3	3.44	3.1	149
M-7 172.6	293.001	1.54	1.15	3.98	0.586	5.09	1.48	1.7	0.0	0.0	11.32	6.3	131
M-7 182.0	295.001	1.45	0.77	2.45	0.367	4.94	0.90	0.0	n.a.	1.4	5.99	3.1	134
M-7 194.9	295.002	1.51	0.88	2.69	0.400	4.39	1.09	1.2	n.a.	1.0	8.77	4.4	137
M-7 200.18	293.002	2.27	1.36	4.67	0.664	5.58	2.44	2.2	0.0	8.0	12.4	27.5	195
M-7 213.0	295.003	4.62	1.53	3.67	0.549	5.46	1.85	1.5	n.a.	3.0	8.23	4.9	113
M-7 223.45	293.003	1.90	1.02	3.22	0.469	4.94	1.13	1.4	0.0	0.0	7.57	5.9	125
M-7 234.78	293.004	1.55	0.88	2.75	0.403	4.07	1.07	0.7	0.1	2.0	9.78	3.6	142
M-7 245.0	293.005	1.65	0.87	3.07	0.448	4.20	0.87	2.0	0.0	0.0	6.07	2.7	147
M-7 265.0	293.006	1.60	0.88	2.95	0.444	4.31	1.00	3.2	0.0	0.0	4.70	2.5	189
M-7 285.1	293.007	1.66	0.92	3.07	0.458	4.95	0.96	2.2	0.0	0.0	5.26	4.2	156
M-7 305.0	293.008	1.57	0.86	2.81	0.428	4.04	1.34	3.0	0.0	0.0	3.70	3.5	165
M-7 315.0	293.009	2.08	1.11	3.25	0.470	5.05	0.94	3.2	0.0	3.0	4.67	2.7	179
M-7 335.0	293.010	1.72	0.81	2.81	0.407	3.94	0.99	2.7	0.0	0.0	5.23	2.5	167
M-7 355.03	293.011	2.22	1.16	3.59	0.551	5.71	1.56	1.8	0.0	0.0	5.40	4.6	156
M-7 375.32	293.012	1.70	0.98	3.35	0.499	4.56	0.99	4.2	1.0	1.0	4.44	2.7	169
M-7 395.37	293.013	2.09	1.12	3.44	0.497	5.33	1.09	3.2	0.9	0.0	5.43	3.1	152
M-7 405.8	293.014	1.36	0.61	1.74	0.259	4.55	0.72	1.8	0.0	0.0	7.36	3.4	169
M-7 415.18	293.015	3.48	1.91	5.02	0.725	8.46	1.56	4.2	1.7	4.0	5.69	4.1	158
M-7 435.0	293.016	1.39	0.92	3.62	0.539	4.68	1.01	2.0	0.0	0.0	5.69	3.5	167
M-7 455.0	293.017	0.97	0.32	1.02	0.163	6.64	0.43	1.6	0.0	4.0	6.72	2.8	159
M-7 479.98	293.018	2.88	1.51	3.76	0.536	6.74	1.08	1.1	0.0	0.0	5.13	3.1	166
M-7 548.57	293.019	2.43	1.16	3.29	0.476	6.13	1.02	2.2	0.0	0.0	4.62	2.8	177
M-7 603.36	293.020	2.47	1.25	3.38	0.485	6.27	0.96	1.6	0.0	2.0	5.07	2.1	169
M-7 662.8	293.021	2.72	1.33	3.57	0.535	7.22	1.03	1.3	0.0	0.0	5.68	2.7	142
M-7 715.4	293.022	2.81	1.44	3.86	0.575	7.94	1.04	2.5	1.5	3.0	6.01	2.8	168
M-8 250.6	293.034	1.16	0.89	2.87	0.424	4.69	1.34	1.1	0.0	1.0	12.4	9.3	188
M-8 285.3A	293.035	3.82	1.35	7.41	1.36	5.74	13.8	1.4	0.4	1.3	3.12	23.9	154
M-8 285.3B	295.010	2.64	0.95	5.66	1.02	5.21	10.5	0.7	n.a.	0.0	0.92	17.2	144
M-8 285.3C	295.011	3.82	1.31	7.61	1.36	5.04	17.9	1.7	n.a.	3.0	1.83	25.5	146
M-8 313.9	293.036	1.30	0.80	2.68	0.398	4.46	0.99	0.8	0.0	0.0	6.64	4.0	159
M-8 393.7	293.037	1.92	1.04	3.18	0.454	5.19	1.01	1.5	0.0	0.0	4.88	2.3	161
M-8 465.8	293.038	1.63	0.83	2.55	0.376	3.85	0.76	2.2	0.5	18	6.09	2.8	163
M-8 491.1	293.039	1.58	0.80	2.54	0.381	4.34	0.82	2.4	0.9	2.1	4.25	3.1	152
M-8 517.1	293.040	1.47	0.80	2.41	0.364	4.39	1.05	1.5	0.3	1.3	4.52	2.5	167
M-10 258.6	293.023	1.01	0.82	2.71	0.401	6.44	1.08	0.9	0.2	0.8	7.46	3.1	161
M-10 274.2	293.024	0.90	0.60	2.06	0.310	7.71	0.86	0.8	0.0	1.0	6.24	2.6	173
M-10 301.8	293.025	1.14	0.78	2.41	0.365	6.44	0.94	0.9	0.0	1.0	7.31	3.0	169
M-10 324.2	293.026	1.03	0.64	1.91	0.285	7.23	0.79	0.7	0.0	1.2	5.31	2.4	182
M-10 346.1	293.027	1.82	0.90	3.07	0.460	8.49	1.14	0.8	0.0	1.7	9.27	3.7	121
M-10 366.8	293.028	1.62	0.88	2.79	0.408	7.89	1.04	1.1	0.0	0.7	8.28	3.6	172
M-10 405.9	293.029	1.21	0.78	2.63	0.407	7.78	1.08	1.1	0.0	1.0	7.23	3.3	163
M-10 434.4	293.030	1.56	1.13	3.90	0.531	6.19	1.60	1.6	0.7	0.0	12.9	5.5	155
M-10 448.9	293.031	1.51	1.12	3.65	0.522	4.81	1.43	1.6	0.4	2.0	9.59	5.0	154
M-10 452.4	293.032	1.25	1.00	3.25	0.468	5.34	1.29	1.8	0.0	8.2	14.7	5.9	171
M-10 465.6	293.033	1.29	1.05	3.47	0.501	4.94	1.29	2.1	0.0	3.2	9.99	7.7	151
M-10 489.5	295.012	1.37	1.23	4.20	0.610	5.42	1.38	1.9	n.a.	1.0	14.6	7.0	112
σ†		0.02	0.02	0.05	0.010	0.06	0.05	0.8	0.8	2	0.12	0.3	.....

*The core number and depth in feet is coded into the sample designation, e.g., M-1 380.05 represents the sample at 380.05 feet depth in core M-1. Letter designations A, B, etc. in sample name (e.g., M-1 380.05A) represent replicate subsamples.

†Estimates of analytical uncertainty for a typical sample (σ = standard deviation). Concentration values for Se, Br, W, Ir, Au are usually at or below detection limits (essentially 2σ) for most samples.

APPENDIX 2. MAJOR ELEMENT DATA FOR BRECCIA SAMPLES

TABLE A2.1. MAJOR ELEMENT COMPOSITIONS OF MATRIX-RICH SAMPLES FROM THE M-1 CORE BY ELECTRON MICROPROBE ANALYSIS OF FUSED BEADS*

	M-1	M-1	M-1	M-1	M-1	M-1	M-1	M-1
Depth (feet)	367.65	390.2	410.5	439.45	459.25	480.2	497.75	516.75
Interval	IMB	IMB	IMB	IMB	IMB	IMB	TZ	TZ
EMP spots	8	8	8	8	8	8	10	8
SiO_2	62.9 ± 2.3	64.8 ± 2.2	63.8 ± 2.5	62.4 ± 1.0	61.8 ± 2.3	61.1 ± 1.7	59.1 ± 1.5	61.7 ± 1.6
TiO_2	0.81 ± 0.11	0.75 ± 0.31	1.07 ± 0.22	0.99 ± 0.27	1.05 ± 0.27	1.05 ± 0.16	0.96 ± 0.17	0.77 ± 0.08
Al_2O_3	15.2 ± 1.0	15.3 ± 2.5	14.9 ± 1.0	15.4 ± 0.9	16.2 ± 1.1	16.0 ± 0.6	16.8 ± 0.4	16.0 ± 0.9
Cr_2O_3	0.01 ± 0.01	0.01 ± 0.01	0.01 ± 0.02	0.01 ± 0.02	0.02 ± 0.02	0.01 ± 0.01	0.02 ± 0.02	0.02 ± 0.02
Fe_2O_3	5.8 ± 0.7	5.0 ± 1.0	6.1 ± 0.6	6.3 ± 0.4	6.3 ± 0.6	6.8 ± 0.4	8.9 ± 0.8	6.5 ± 0.5
MnO	0.11 ± 0.02	0.08 ± 0.03	0.10 ± 0.02	0.12 ± 0.02	0.11 ± 0.02	0.09 ± 0.04	0.10 ± 0.01	0.09 ± 0.01
MgO	3.69 ± 0.38	3.04 ± 0.54	2.85 ± 0.24	3.21 ± 0.13	2.90 ± 0.34	3.01 ± 0.18	4.10 ± 0.36	3.50 ± 0.24
CaO	3.52 ± 0.46	2.53 ± 0.45	3.47 ± 0.50	3.62 ± 0.19	4.61 ± 0.44	4.62 ± 0.26	3.07 ± 0.27	3.61 ± 0.33
Na_2O	3.15 ± 0.12	3.12 ± 0.41	3.43 ± 0.24	3.42 ± 0.19	3.44 ± 0.20	3.50 ± 0.16	4.07 ± 0.27	4.11 ± 0.24
K_2O	3.05 ± 0.23	3.64 ± 0.16	2.05 ± 0.15	3.32 ± 0.27	2.55 ± 0.18	2.45 ± 0.15	2.23 ± 0.24	2.67 ± 0.57
P_2O_5	0.29 ± 0.16	0.17 ± 0.13	0.19 ± 0.08	0.21 ± 0.07	0.22 ± 0.10	0.27 ± 0.13	0.19 ± 0.05	0.15 ± 0.05
Total	98.4	98.5	99.0	99.0	99.2	99.0	99.5	99.1

	M-1	M-1	M-1	M-1	M-1	M-1	EMPA	M-1 Averages		
Depth (feet)	544.0	573.65	594.07	614.45	642.42	692.5	Average			
Interval	SB	SB	SB	SB	SB	SB	Counting	IMB	TZ	SB
EMP spots	10	8	11	8	8	10	Statistics			
SiO_2	60.0 ± 1.1	58.6 ± 1.5	58.8 ± 2.8	60.1 ± 3.0	58.2 ± 2.6	59.1 ± 2.1	0.19	62.8	60.4	59.1
TiO_2	0.74 ± 0.14	0.90 ± 0.20	0.72 ± 0.20	0.83 ± 0.25	1.37 ± 0.28	0.92 ± 0.05	0.02	0.95	0.86	0.91
Al_2O_3	17.1 ± 0.9	17.3 ± 1.1	16.3 ± 1.0	16.4 ± 1.2	15.7 ± 0.8	16.1 ± 1.0	0.07	15.5	16.4	16.5
Cr_2O_3	<0.01 ± 0.01	0.02 ± 0.01	0.01 ± 0.02	0.02 ± 0.01	0.02 ± 0.02	0.01 ± 0.01	0.02	0.01	0.02	0.01
Fe_2O_3	6.1 ± 0.7	6.9 ± 0.6	7.4 ± 1.5	6.3 ± 1.0	8.3 ± 0.9	7.3 ± 0.4	0.08	6.1	7.7	7.0
MnO	0.09 ± 0.02	0.09 ± 0.02	0.11 ± 0.03	0.10 ± 0.03	0.13 ± 0.03	0.11 ± 0.02	0.02	0.10	0.09	0.11
MgO	3.55 ± 0.59	3.75 ± 0.34	3.65 ± 0.55	3.51 ± 0.49	4.06 ± 0.38	3.88 ± 0.31	0.02	3.12	3.80	3.73
CaO	5.17 ± 0.38	4.95 ± 0.30	4.96 ± 0.43	5.68 ± 0.64	5.16 ± 0.36	5.07 ± 0.37	0.03	3.73	3.34	5.17
Na_2O	4.58 ± 0.21	4.84 ± 0.23	4.64 ± 0.18	4.61 ± 0.14	4.39 ± 0.17	4.55 ± 0.09	0.03	3.34	4.09	4.60
K_2O	1.98 ± 0.08	2.11 ± 0.14	1.87 ± 0.19	1.95 ± 0.21	1.92 ± 0.20	2.16 ± 0.16	0.02	3.01	2.45	2.00
P_2O_5	0.16 ± 0.11	0.18 ± 0.07	0.18 ± 0.06	0.22 ± 0.09	0.25 ± 0.06	0.19 ± 0.08	0.02	0.22	0.17	0.20
Total	99.5	99.6	98.6	99.7	99.5	99.4		98.9	99.3	99.4

*Analytical uncertainties represents one-sigma spot-to-spot standard deviations. Total Fe as Fe_2O_3. Beam size - 40 micrometers. Abbreviations: IMB = impact-melt breccia; TZ = transition zone between IMB and SB intervals; SB = fragmental-matrix suevitic breccia. Note: These were fused at high temperature, therefore the fused-bead analyses are nominally anhydrous.

TABLE A2.2. COMPOSITIONS OF IMPACT-MELT BRECCIA (MATRIX-RICH) AND IMPACT-MELT BRECCIA VEIN IN CRYSTALLINE BASEMENT ROCKS*

Core	M-1	M-1	M-7
Depth (feet)	367.65	439.5	475.6
Rock Type	Impact-Melt Breccia (IMB)	Impact-Melt Breccia (IMB)	IMB Dike in Central-Peak Crystalline Rock
X-RAY FLUORESCENCE (XRF)			
cg/g			
SiO_2	63.28 ± 0.11	63.36 ± 0.11	43.43 ± 0.09
TiO_2	0.79 ± 0.01	0.87 ± 0.01	3.77 ± 0.03
Al_2O_3	15.96 ± 0.07	14.94 ± 0.07	14.18 ± 0.07
Fe_2O_3(t)	5.59 ± 0.02	5.84 ± 0.02	14.78 ± 0.04
MnO	0.09 ± 0.00	0.10 ± 0.00	0.13 ± 0.01
MgO	3.42 ± 0.04	2.70 ± 0.04	5.26 ± 0.05
CaO	3.03 ± 0.02	3.18 ± 0.02	7.13 ± 0.03
Na_2O	2.90 ± 0.07	3.50 ± 0.07	3.49 ± 0.07
K_2O	2.87 ± 0.02	3.17 ± 0.02	1.20 ± 0.01
P_2O_5	0.18 ± 0.01	0.19 ± 0.01	1.93 ± 0.02
L.O.I.	2.22	2.17	4.28
Total	100.3	100.0	99.6
INSTRUMENTAL NEUTRON ACTIVATION ANALYSIS (INAA)			
Fe_2O_3(t)	6.01 ± 0.06	5.91 ± 0.06	14.74 ± 0.14
CaO	3.50 ± 0.30	3.17 ± 0.30	7.10 ± 0.47
Na_2O	3.02 ± 0.03	3.43 ± 0.03	3.60 ± 0.04
K_2O	2.8 ± 0.5	3.3 ± 0.5	1.1 ± 0.9
μg/g (except where noted)			
Sc	13.4 ± 0.1	13.3 ± 0.1	25.3 ± 0.3
Cr	75.1 ± 0.8	57.4 ± 0.6	53.8 ± 0.9
Co	17.1 ± 0.2	15.2 ± 0.1	39.6 ± 0.4
Ni	45 ± 12	25 ± 10	60 ± 50
Zn	81 ± 2	62 ± 2	179 ± 5
As	1.6 ± 0.3	1.1 ± 0.3	<6
Se	0.2 ± 0.25	<0.6	<1.9
Br	0.4 ± 0.2	0.4 ± 0.2	<2.2
Rb	114 ± 2	118 ± 2	33 ± 3
Sr	244 ± 15	237 ± 13	370 ± 50
Zr	168 ± 17	220 ± 16	440 ± 40
Sb	0.20 ± 0.02	0.10 ± 0.02	0.04 ± 0.06
Cs	1.51 ± 0.03	1.73 ± 0.03	0.73 ± 0.06
Ba	659 ± 12	711 ± 11	703 ± 20
La	33.3 ± 0.3	37.2 ± 0.4	78.5 ± 0.79
Ce	65.9 ± 0.7	75.0 ± 0.8	173 ± 1.7
Nd	28 ± 2	32 ± 2	93 ± 5.1
Sm	6.10 ± 0.06	6.61 ± 0.07	19.24 ± 0.19
Eu	1.28 ± 0.02	1.26 ± 0.02	4.79 ± 0.05
Tb	1.03 ± 0.02	1.01 ± 0.02	2.49 ± 0.04
Yb	4.20 ± 0.04	3.81 ± 0.04	5.76 ± 0.06
Lu	0.61 ± 0.01	0.58 ± 0.01	0.84 ± 0.01
Hf	4.88 ± 0.05	6.15 ± 0.07	10.96 ± 0.13
Ta	1.58 ± 0.03	1.46 ± 0.03	1.80 ± 0.05
Au (ng/g)	<5	<3	<10
Th	9.28 ± 0.09	10.0 ± 0.1	6.11 ± 0.07
U	7.98 ± 0.2	6.4 ± 0.2	2.46 ± 0.18
Mass, INAA (g)	0.205	0.761	0.224
Approximate mass of powdered sample (g):	1	2	47

Note: Oxide concentrations given in cg/g (wt.%), Au in ng/g (ppb), and all others in μg/g (ppm).

*Analytical uncertainty reflects counting statistics (one sigma) only. Fe_2O_3(t) = total Fe as Fe_2O_3. Samples M-1 367.65 and M-1 439.5 are clast-bearing, low-porosity impact-melt breccias; lithic clasts are shocked to partially melted; quartz clasts are strongly shocked (toasted) or recrystallized; all clasts are embayed or surrounded by reaction halos; matrix is green, very fine grained, chlorite-rich. Sample M-7 475.6 is a clast-bearing impact-melt-breccia dike at least 10 cm across in gneissic basement rocks just below contact with "suevitic breccia"; matrix is brown, flow-textured, isotropic, and glassy to very finely devitrified.

APPENDIX 3. COMPOSITIONS OF TARGET ROCKS

TABLE A3.1. COMPOSITIONS OF GRANITE AND PEGMATITIC GRANITE, MANSON TARGET ROCKS*

Core	2-A	2-A	M-1	2-A	2-A	Manson	Manson
Depth (feet)	460.7	472.9	355.9	247.9	446.4	Granite	Pegmatitic-Granite
Rock Type	Granite	Granite	Granite Clast	Pegmatitic Granite	Pegmatitic Granite	Average	Average
X-RAY FLUORESCENCE (XRF)							
cg/g %							
SiO_2	76.05 ± 0.13	71.78 ± 0.12	74.72 ± 0.12	71.84 ± 0.12	67.02 ± 0.12	74.18	69.44
TiO_2	0.09 ± 0.005	0.12 ± 0.006	0.06 ± 0.005	0.11 ± 0.006	0.08 ± 0.005	0.09	0.09
Al_2O_3	13.09 ± 0.07	13.85 ± 0.07	12.73 ± 0.07	13.56 ± 0.07	16.47 ± 0.07	13.22	15.01
Fe_2O_3(t)	0.87 ± 0.01	1.05 ± 0.01	1.47 ± 0.01	0.96 ± 0.01	0.66 ± 0.01	1.13	0.81
MnO	0.012 ± 0.002	0.020 ± 0.003	0.021 ± 0.003	0.011 ± 0.003	0.010 ± 0.003	0.02	0.01
MgO	0.26 ± 0.03	0.23 ± 0.03	0.98 ± 0.03	0.22 ± 0.03	0.23 ± 0.03	0.49	0.23
CaO	0.76 ± 0.01	2.07 ± 0.01	0.66 ± 0.01	0.43 ± 0.01	0.70 ± 0.01	1.16	0.57
Na_2O	3.70 ± 0.07	3.30 ± 0.07	2.97 ± 0.07	1.52 ± 0.06	1.30 ± 0.06	3.32	1.41
K_2O	5.04 ± 0.03	6.25 ± 0.03	5.57 ± 0.03	9.49 ± 0.04	12.77 ± 0.05	5.62	11.13
P_2O_5	0.04 ± 0.01	0.10 ± 0.01	0.06 ± 0.01	0.10 ± 0.01	0.33 ± 0.01	0.07	0.21
L.O.I.	0.5	1.7	1.2	1.5	0.7	1.1	1.1
Total	100.4	100.5	100.4	99.7	100.2	100.4	100.0
INSTRUMENTAL NEUTRON ACTIVATION ANALYSIS (INAA)							
Fe_2O_3(t)	0.85 ± 0.01	1.05 ± 0.01	1.44 ± 0.01	0.93 ± 0.01	0.67 ± 0.01	1.11	0.80
CaO	0.71 ± 0.15	2.26 ± 0.19	0.50 ± 0.13	0.40 ± 0.42	0.71 ± 0.12	1.2	0.6
Na_2O	3.71 ± 0.04	3.22 ± 0.03	2.90 ± 0.03	1.51 ± 0.01	1.30 ± 0.01	3.28	1.40
K_2O	5.5 ± 0.7	6.4 ± 0.8	5.7 ± 0.7	9.2 ± 1.1	12.9 ± 1.1	5.9	11.1
µg/g (except where noted)							
Sc	2.30 ± 0.02	2.68 ± 0.03	0.66 ± 0.01	3.02 ± 0.03	1.57 ± 0.02	1.9	2.3
Cr	1.11 ± 0.18	1.21 ± 0.16	0.80 ± 0.21	0.5 ± 0.5	0.80 ± 0.20	1.0	0.7
Co	1.04 ± 0.02	0.89 ± 0.01	3.58 ± 0.04	2.03 ± 0.03	1.03 ± 0.02	1.8	1.5
Ni	<18	<16	<18	<25	<17	1.7	1.5
Zn	19 ± 1	28 ± 1	14 ± 1	19 ± 1	14 ± 1	21	16
As	0.25 ± 0.18	<0.5	1.6 ± 0.2	1.7 ± 0.4	<0.6	<1	<1
Se	<0.5	<0.24	<0.6	<0.6	<0.4	<0.5	<0.5
Br	<0.4	0.3 ± 0.1	0.3 ± 0.1	0.5 ± 0.2	<0.4	0.2	0.3
Rb	139 ± 2	183 ± 2	175 ± 2	281 ± 3	301 ± 3	166	291
Sr	130 ±13	129 ± 8	121 ±10	149 ±15	158 ±13	127	153
Zr	153 ±11	85 ± 8	234 ±13	31 ±15	23 ± 8	157	27
Sb	<0.02	<0.02	0.14 ± 0.01	0.08 ± 0.02	<0.02	0.05	0.04
Cs	0.64 ± 0.02	0.51 ± 0.01	0.78 ± 0.02	1.23 ± 0.03	1.03 ± 0.02	0.65	1.13
Ba	564 ±11	988 ±14	451 ±11	934 ±15	2,010 ±20	668	1,472
La	3.76 ± 0.04	21.7 ± 0.2	12.9 ± 0.1	241 ± 3	17.0 ± 0.2	12.8	129
Ce	7.0 ± 0.2	45.6 ± 0.5	29.8 ± 0.3	504 ± 6	36.5 ± 0.4	27.5	270
Nd	2.3 ± 1.3	18.2 ± 1.6	12.5 ± 1.6	201 ± 7	16.5 ± 1.3	11.0	109
Sm	0.90 ± 0.01	3.56 ± 0.04	3.86 ± 0.08	39.7 ± 0.4	4.14 ± 0.04	2.77	21.92
Eu	0.84 ± 0.01	1.26 ± 0.01	0.38 ± 0.01	1.65 ± 0.02	1.32 ± 0.01	0.83	1.49
Tb	0.16 ± 0.01	0.35 ± 0.01	0.67 ± 0.02	2.87 ± 0.07	0.73 ± 0.01	0.39	1.80
Yb	0.50 ± 0.02	0.55 ± 0.01	2.79 ± 0.03	1.86 ± 0.04	1.42 ± 0.02	1.28	1.64

TABLE A3.1. COMPOSITIONS OF GRANITE AND PEGMATITIC GRANITE, MANSON TARGET ROCKS* (continued)

Core	2-A	2-A	M-1	2-A	2-A	Manson	Manson
Depth (feet)	460.7	472.9	355.9	247.9	446.4	Granite	Pegmatitic-Granite
Rock Type	Granite	Granite	Granite Clast	Pegmatitic Granite	Pegmatitic Granite	Average	Average
INSTRUMENTAL NEUTRON ACTIVATION ANALYSIS (INAA) (continued)							
μg/g (except where noted)							
Lu	0.089 ± 0.005	0.078 ± 0.004	0.440 ± 0.010	0.286 ± 0.007	0.189 ± 0.004	0.20	0.24
Hf	5.14 ± 0.06	2.80 ± 0.03	8.86 ± 0.09	1.49 ± 0.04	0.70 ± 0.02	5.60	1.09
Ta	0.30 ± 0.01	0.34 ± 0.01	0.50 ± 0.02	0.71 ± 0.02	0.28 ± 0.01	0.38	0.49
Au (ng/g)	<2.5	2.8 ± 1.0	<5	6.5 ± 1.4	1.8 ± 0.8	<2.5	4.2
Th	2.35 ± 0.03	10.6 ± 0.1	32.5 ± 0.3	233 ± 3	5.87 ± 0.06	15.2	119
U	2.7 ± 0.1	11.1 ± 0.2	35.9 ± 0.6	25.5 ± 0.4	1.75 ± 0.06	16.6	13.6
Mass, INAA (g)	0.159	0.194	0.208	0.169	0.178		
Approximate mass of powdered sample (g):	72	97	48	88	90		

Note: Oxide concentrations in cg/g (wt.%), Au in ng/g (ppb) and all others in μg/g (ppm).

*Analytical uncertainty reflects counting statistics (one sigma) only. $Fe_2O_3(t)$ = total Fe as Fe_2O_3. Sample 2-A 460.7 is medium-grained Qtz-Kfs-Alb-chlorite granite; Qtz and feldspars strongly shocked, plagioclase is altered. Sample 2-A 472.9 is fine-grained Qtz-Kfs-Alb-Bio leucogranite, weakly foliated; strongly shocked Qtz, pervasively altered feldspars, chlorite replaces biotite; epidote, calcite, sulfide secondary mineralization. Sample M-1 355.9 is a large, strongly shocked, partially melted granite clast from impact-melt-breccia interval. Feldspars are flow-textured and partially isotropic, quartz is granoblastic (recrystallized), mafic mineral partially dissolved and replaced by chlorite. Sample 2-A 247.9, from a large block of crystalline rock in breccia, is coarse (0.5 to 2 cm), Qtz-Kfs granite, strongly shocked, "toasted quartz," partially melted feldspar; accessory Bio strongly shocked, partly altered. Sample 2-A 446.4 is coarse, graphic Qtz-Kfs-granite; Qtz is milky-white, Kfs is reddish-orange, accessory mafics unevenly disseminated. Granite average is the mean of 2-A 460.7, 2-A 472.9, and M-1 355.9; pegmatitic-granite average is mean of 2-A 247.9 and 2-A 446.4. Average Ni, Br, Sb concentrations based on low-precision data.

TABLE A3.2. COMPOSITIONS OF GNEISS AND DIABASE, MANSON TARGET ROCKS*

Core	2-A	M-7	M-7	2-A	Hbd-Bio
Depth (feet)	449.6	493.6	728.4	251.7	Gneiss
Rock Type	Hbd-Bio Gneiss	Hbd-Bio Gneiss	Hbd-Bio Gneiss	Diabase	Average
X-RAY FLUORESCENCE (XRF)					
cg/g					
SiO_2	49.24 ± 0.10	61.56 ± 0.11	54.40 ± 0.10	40.26 ± 0.09	55.06
TiO_2	1.51 ± 0.016	0.67 ± 0.010	0.94 ± 0.012	5.38 ± 0.05	1.04
Al_2O_3	18.35 ± 0.08	18.92 ± 0.08	17.71 ± 0.08	13.03 ± 0.07	18.33
Fe_2O_3(t)	11.94 ± 0.03	4.26 ± 0.01	8.19 ± 0.02	20.37 ± 0.05	8.13
MnO	0.20 ± 0.006	0.05 ± 0.003	0.12 ± 0.004	0.31 ± 0.01	0.12
MgO	4.71 ± 0.04	1.84 ± 0.03	4.55 ± 0.04	5.01 ± 0.05	3.70
CaO	5.48 ± 0.02	4.79 ± 0.02	7.17 ± 0.03	4.78 ± 0.02	5.81
Na_2O	4.14 ± 0.07	4.94 ± 0.08	4.09 ± 0.08	2.94 ± 0.07	4.39
K_2O	2.13 ± 0.02	1.51 ± 0.01	1.64 ± 0.02	1.64 ± 0.02	1.76
P_2O_5	0.41 ± 0.01	0.19 ± 0.01	0.17 ± 0.01	2.79 ± 0.03	0.26
L.O.I.	2.2	1.3	1.2	3.2	1.5
Total	100.3	100.0	100.1	99.7	100.1
INSTRUMENTAL NEUTRON ACTIVATION ANALYSIS (INAA)					
Fe_2O_3(t)	11.78 ± 0.12	4.07 ± 0.04	8.15 ± 0.08	20.1 ± 0.2	8.00
CaO	5.9 ± 0.4	4.9 ± 0.2	7.2 ± 0.4	5.6 ± 0.6	6.0
Na_2O	4.17 ± 0.04	4.84 ± 0.05	4.02 ± 0.04	2.86 ± 0.03	4.34
K_2O	1.8 ± 0.7	1.8 ± 0.7	1.6 ± 0.5	<3 ± 0.7	1.7
µg/g (except where noted)					
Sc	27.7 ± 0.3	1.76 ± 0.02	22.1 ± 0.2	31.4 ± 0.3	17.2
Cr	105 ± 1	8.60 ± 0.28	49.3 ± 0.7	47.9 ± 1.4	54.3
Co	27.1 ± 0.3	9.81 ± 0.10	26.5 ± 0.3	55.0 ± 0.6	21.1
Ni	<100	17 ± 13	40 ± 30	80 ± 60	29
Zn	227 ± 4	53.1 ± 1.4	101 ± 3	255 ± 7	127
As	<1.8	<0.7	<1.0	1.7 ± 0.6	<1
Se	<0.9	<0.4	n.d.	<1.6	<0.5
Br	<0.9	0.8 ± 0.2	0.5 ± 0.2	<0.9	0.5
Rb	124 ± 4	46 ± 2	46 ± 3	43 ± 6	72
Sr	290 ± 30	722 ± 17	600 ± 30	250 ± 50	537
Zr	200 ± 30	383 ± 14	180 ± 30	610 ± 60	254
Sb	<0.09	<0.05	<0.07	<0.24	<0.05
Cs	4.26 ± 0.08	2.92 ± 0.03	1.66 ± 0.06	1.01 ± 0.09	2.95
Ba	395 ± 20	840 ± 13	750 ± 20	680 ± 30	662
La	34.1 ± 0.4	20.4 ± 0.2	28.7 ± 0.3	92.9 ± 0.9	27.7
Ce	65.9 ± 0.7	37.4 ± 0.4	59.1 ± 0.6	205 ± 2.1	54.1
Nd	26 ± 4	15.3 ± 1.6	27 ± 4	109 ± 9	22.8
Sm	6.04 ± 0.06	2.41 ± 0.03	5.27 ± 0.05	24.1 ± 0.3	4.57
Eu	1.40 ± 0.03	1.02 ± 0.01	1.49 ± 0.03	5.12 ± 0.08	1.30
Tb	0.82 ± 0.03	0.23 ± 0.01	0.66 ± 0.02	3.05 ± 0.07	0.57
Yb	2.48 ± 0.05	0.93 ± 0.02	2.16 ± 0.04	6.93 ± 0.09	1.86
Lu	0.359 ± 0.011	0.162 ± 0.005	0.328 ± 0.009	0.99 ± 0.02	0.28
Hf	4.68 ± 0.09	9.19 ± 0.09	4.31 ± 0.07	14.30 ± 0.21	6.06

TABLE A3.2. COMPOSITIONS OF GNEISS AND DIABASE, MANSON TARGET ROCKS* (continued)

Core	2-A	M-7	M-7	2-A	Hbd-Bio
Depth (feet)	449.6	493.6	728.4	251.7	Gneiss
Rock Type	Hbd-Bio Gneiss	Hbd-Bio Gneiss	Hbd-Bio Gneiss	Diabase	Average
		INSTRUMENTAL NEUTRON ACTIVATION ANALYSIS (INAA)			
μg/g (except where noted)					
Ta	1.21 ± 0.05	0.65 ± 0.02	0.48 ± 0.03	2.02 ± 0.09	0.78
Au (ng/g)	<6	<7	<8	<8	<4
Th	3.72 ± 0.06	4.49 ± 0.05	2.94 ± 0.05	6.86 ± 0.10	3.7
U	2.37 ± 0.17	2.66 ± 0.12	1.48 ± 0.11	7.5 ± 0.3	2.2
Mass, INAA (g)	0.190	0.220	0.221	0.197	
Approximate mass of powdered sample (g):	37	60	54	27	

Oxide concentrations given in cg/g (wt.%), Au in ng/g (ppb), and all others in μg/g (ppm).
Analytical uncertainty - counting statistics (one sigma) only. $Fe_2O_3(t)$ = total Fe as Fe_2O_3. Sample 2-A 449.6 is a fine-grained, weakly foliated, granular to granoblastic Bio-Hbd-Plag-Qtz gneiss with shocked quartz, partly isotropic biotite, altered plagioclase, and minor magnetite and sphene. Sample M-7 493.6 is leucocratic, medium-grained, granular to banded Bio-Hbd-Plg-Kfs-Qtz-Mgt gneiss with weak foliation, shocked quartz, partly to strongly altered feldspars. Sample M-7 728.4 is dark, medium- to coarse-grained, banded Hbd-Plg-Qtz-Bio gneiss with moderate foliation, shocked quartz, altered plagioclase, and crushed zones; accessory sphene. Sample 2-A 251.7 is a large clast of fine-grained, intergranular-subophitic diabase; altered, with abundant oxides and phosphate. Gneiss average is the mean of 2-A 449.6, M-7 493.6, and M-7 728.4.

TABLE A3.3. COMPOSITIONS OF SHALE CLAST FROM THE M-1 CORE AND "RED CLASTICS" FROM THE AMOCO M. G. EISCHEID #1 WELL*

Core Depth (feet) Rock Type	M-7 210.0 Shale Clast in Impact-melt Breccia	Eischeid E 8,837.5 Arkosic Sandstone	Eischeid D 11,390.2 Red Mudstone	Eischeid C 15,097.0 Black Shale	Eischeid Red-Clastics Average
			X-Ray Fluorescence (XRF)		
cg/g					
SiO_2	54.42 ± 0.10	83.30 ± 0.13	68.68 ± 0.12	57.49 ± 0.10	69.83
TiO_2	1.04 ± 0.01	0.35 ± 0.01	1.05 ± 0.01	1.08 ± 0.01	0.83
Al_2O_3	21.74 ± 0.09	7.16 ± 0.05	11.52 ± 0.06	16.57 ± 0.07	11.75
Fe_2O_3(t)	7.31 ± 0.02	2.58 ± 0.01	4.18 ± 0.01	7.67 ± 0.02	4.81
MnO	0.026 ± 0.00	0.033 ± 0.00	0.07 ± 0.00	0.06 ± 0.00	0.06
MgO	2.31 ± 0.03	0.43 ± 0.03	1.62 ± 0.03	4.70 ± 0.04	2.25
CaO	0.57 ± 0.01	1.31 ± 0.01	4.10 ± 0.02	1.46 ± 0.01	2.29
Na_2O	0.48 ± 0.05	0.80 ± 0.05	2.34 ± 0.06	1.78 ± 0.06	1.64
K_2O	4.11 ± 0.03	2.78 ± 0.02	2.83 ± 0.02	3.71 ± 0.02	3.11
P_2O_5	0.10 ± 0.01	0.09 ± 0.01	0.24 ± 0.01	0.14 ± 0.01	0.15
L.O.I.	8.03	1.5	3.77	5.38	3.55
Total	100.1	100.3	100.4	100.0	100.3
			Instrumental Neutron Activation Analysis (INAA)		
Fe_2O_3(t)	7.18 ± 0.07	2.44 ± 0.02	4.04 ± 0.04	7.55 ± 0.08	4.68
CaO	<0.8	1.24 ± 0.11	4.5 ± 0.3	1.7 ± 0.4	2.5
Na_2O	0.44 ± 0.01	0.79 ± 0.01	2.25 ± 0.02	1.71 ± 0.02	1.58
K_2O	4.1 ± 0.5	2.9 ± 0.4	3.1 ± 0.6	4.0 ± 1.0	3.3
μg/g (except where noted)					
Sc	18.2 ± 0.2	4.03 ± 0.04	10.0 ± 0.1	18.8 ± 0.2	10.9
Cr	116.8 ± 1.2	14.4 ± 0.3	37.0 ± 0.7	75.1 ± 1.0	42.2
Co	16.7 ± 0.2	4.68 ± 0.05	9.04 ± 0.09	27.1 ± 0.3	13.6
Ni	34 ± 19	<30	<60	60 ± 30	24
Zn	64 ± 2.2	27 ± 1	70 ± 2	124 ± 4	74
As	3.9 ± 0.5	12.4 ± 0.2	7.9 ± 0.4	28.8 ± 0.8	16.4
Se	<1.0	<0.3	<0.7	0.3 ± 0.4	<0.5
Br	<1.7	4.4 ± 0.4	1.4 ± 0.2	2.0 ± 0.4	2.6
Rb	243 ± 3	92 ± 1	90 ± 2	147 ± 5	109
Sr	79 ± 20	99 ± 12	156 ± 30	133 ± 30	129
Zr	230 ± 19	126 ± 10	581 ± 30	180 ± 40	295
Sb	0.17 ± 0.02	0.82 ± 0.02	0.90 ± 0.03	3.48 ± 0.07	1.73
Cs	13.80 ± 0.14	1.69 ± 0.02	2.87 ± 0.05	6.88 ± 0.09	3.81
Ba	303 ± 11	453 ± 8	438 ± 13	430 ± 20	440
La	64.1 ± 0.6	20.2 ± 0.2	44.1 ± 0.4	37.0 ± 0.4	33.8
Ce	128 ± 2	42.3 ± 0.4	94.8 ± 1.0	77.8 ± 0.8	71.6
Nd	51 ± 3	21.1 ± 1.4	45 ± 4	34 ± 5	33.4
Sm	8.68 ± 0.09	4.51 ± 0.04	9.36 ± 0.09	8.35 ± 0.08	7.41
Eu	1.36 ± 0.02	0.95 ± 0.01	1.68 ± 0.03	1.50 ± 0.03	1.38
Tb	0.96 ± 0.02	0.67 ± 0.01	1.47 ± 0.03	1.20 ± 0.03	1.11
Yb	3.06 ± 0.03	2.34 ± 0.02	5.47 ± 0.06	4.14 ± 0.06	3.99

TABLE A3.3. COMPOSITIONS OF SHALE CLAST FROM THE M-1 CORE AND "RED CLASTICS" FROM THE AMOCO M. G. EISCHEID #1 WELL* (continued)

Core	M-7	Eischeid E	Eischeid D	Eischeid C	Eischeid
Depth (feet)	210.0	8,837.5	11,390.2	15,097.0	Red-
Rock Type	Shale Clast in Impact-melt Breccia	Arkosic Sandstone	Red Mudstone	Black Shale	Clastics Average
		INSTRUMENTAL NEUTRON ACTIVATION ANALYSIS (INAA)			
μg/g (except where noted)					
Lu	0.46 ± 0.01	0.344 ± 0.005	0.83 ± 0.01	0.62 ± 0.01	0.60
Hf	6.39 ± 0.06	3.72 ± 0.04	15.3 ± 0.2	5.65 ± 0.11	8.24
Ta	3.55 ± 0.05	0.41 ± 0.01	1.08 ± 0.03	1.11 ± 0.05	0.87
Au (ng/g)	<7	0.4 ± 0.7	1.4 ± 1.4	5.4 ± 2.2	2.4
Th	16.13 ± 0.16	4.51 ± 0.04	11.6 ± 0.12	12.6 ± 0.13	9.5
U	8.84 ± 0.18	1.76 ± 0.06	4.29 ± 0.14	5.9 ± 0.2	4.0
Mass, INAA (g)	0.167	0.451	0.283	0.458	
Approximate mass of powdered sample (g):	23	6	3	3	

Oxide concentrations given in cg/g (wt.%), Au in ng/g (ppb), and all others in μg/g (ppm).
*Analytical uncertainty reflects counting statistics (one sigma) only. $Fe_2O_3(t)$ = total Fe as Fe_2O_3. Sample M-7 210.0 is a large shale clast in impact-melt breccia. Sample Eischeid 8,837.5 is arkosic red sandstone from Unit E (7,020 to 10,510 feet) of the Keweenawan "upper Red Clastic" sequence. Sample Eischeid 11,390.2 is red mudstone from Unit D (10,510 to 14,980 feet), and Eischeid 15,097.0 is black shale from Unit C (14,980 to 16,450 feet); both are from the Keweenawan "lower Red Clastic" sequence (Witzke, 1990). "Eischeid Red-Clastics average" is the mean of E-8,837.5, 11,390.2, 15,097.0.

REFERENCES CITED

Anders, E., and Grevesse, N., 1989, Abundances of the elements: Meteoritic and solar: Geochimica et Cosmochimica Acta, v. 53, p. 197–214.

Anderson, R. R., and Hartung, J. B., 1992, The Manson impact structure; its contribution to impact materials observed at the Cretaceous/Tertiary boundary, *in* Proceedings of Lunar and Planetary Science, Houston, March 1991, Volume 22: Houston, Texas, Lunar and Planetary Institute, p. 101–110.

Anderson, R. R., Witzke, B. J., Hartung, J. B., Shoemaker, D. J., and Roddy, D. J., 1993, Descriptions and preliminary interpretations of cores recovered from the Manson impact structure (Iowa) [abs.]: Houston, Lunar and Planetary Institute, Lunar and Planetary Science XXIV, p. 35–36.

Bell, M. S., Reagan, M. K., Anderson, R. R., and Foster, C. T., Jr., 1993, Petrography and preliminary interpretations of the crystalline breccias from the Manson M-1 core [abs.]: Houston, Lunar and Planetary Institute, Lunar and Planetary Science XXIV, p. 87–88.

Boynton, W. V., Baedecker, P. A., Chou, C. -L., Robinson, K. L., and Wasson, J. T., 1975, Mixing and transport of lunar surface materials: Evidence obtained by the determination of lithophile, siderophile, and volatile elements, *in* Proceedings, Lunar Science Conference, 6th, Houston, Geochimica et Cosmochimica Acta, Supplement 6: New York, Pergamon Press, p. 2241–2259.

Couture, R. A., Smith, M. S., and Dymek, R. F., 1993, X-ray fluorescence analysis of silicate rocks using fused glass disk and side-window Rh source tube: Accuracy, precision, and reproducibility: Chemical Geology, v. 110, p. 315–328.

Floran, R. J., Grieve, R. A. F., Phinney, W. C., Warner, J. L., Simonds, C. H., Blanchard, D. P., and Dence, M. R., 1978, Manicouagan impact, Quebec, 1, stratigraphy, petrology, and chemistry: Journal of Geophysical Research, v. 83, p. 2737–2759.

Grieve, R. A. F., Dence, M. R., and Robertson, P. B., 1977, Cratering processes: As interpreted from the occurrence of impact melts, *in* Roddy, D. J., Pepin, R. O., and Merrill, R. B., eds., Impact and explosion cratering: New York, Pergamon Press, p. 791–814.

Gromet, L. P., Dymek, R. F., Haskin, L. A., and Korotev, R. L., 1984, The "North American shale composite": Its compilation, major and trace element characteristics: Geochimica et Cosmochimica Acta, v. 48, p. 2469–2482.

Hartung, J. B., and Anderson, R. R., 1988, A compilation of information and data on the Manson impact structure:. Lunar and Planetary Institute Technical Report No. 88–08, 32 p.

Izett, G. A., Reynolds, R. L., Rosenbaum, J. G., and Nishi, J. M., 1993, A discontinuous melt sheet in the Manson impact structure [abs.]: Houston, Lunar and Planetary Institute, Lunar and Planetary Science XXIV, p. 705–706.

Kane, J. S., Arbogast, B., and Leventhal, J., 1990, Characterization of Devonian Ohio shale SDO-1 as a USGS geochemical reference standard: Geostandards Newsletter, v. 14, p. 169–196.

Koeberl, C., and Hartung, J. B., 1992, Geochemistry of Manson impact structure rocks: Target rocks, impact glasses, and microbreccias, *in* Proceedings of Lunar and Planetary Science, Houston, March 1991, Volume 22: Houston, Texas, Lunar and Planetary Institute, p. 111–126.

Korotev, R. L., 1991, Geochemical stratigraphy of two regolith cores from the Central Highlands of the Moon, *in* Proceedings of Lunar and Planetary Science, Houston, March 1990, Volume 21: Houston, Texas, Lunar and Planetary Institute, p. 229–289.

Korotev, R. L., 1994, Compositional variation in Apollo 16 impact-melt breccias and inferences for the geology and bombardment history of the Central Highlands of the Moon: Geochimica et Cosmochimica Acta, v. 58, p. 3931–3969.

McCarville, P., 1994, Post-impact hydrothermal alteration of the Manson impact structure, Manson, Iowa, [M.S. thesis]: Albuquerque, University of New Mexico, 186 p.

Phinney, W. C., and Simonds, C. H., 1977, Dynamical implications of the petrology and distribution of impact melt rocks, *in* Roddy, D. J., Pepin, R. O., and Merrill, R. B., eds., Impact and explosion cratering: New York, Pergamon Press, p. 771–790.

Reagan, M. K., Foster, C. T., Jr., and Bell, M. S., 1994, Preferential feldspar comminution in melt-rich breccias from the Manson impact structure:

Geological Society of America Abstracts with Programs, v. 26, p. A-338.

Reimold, W. U., 1982, The Lappajärvi meteorite crater, Finland: petrography, Rb-Sr, major and trace element geochemistry if the impact melt and basement rocks: Geochimica et Cosmochimica Acta, v. 46, p. 1203–1225.

Rockow, K. M., Korotev, R. L., Jolliff, B. L., and Haskin, L. A., 1994, Compositional differences between impact-melt breccias of the North and South Massifs at Apollo 17 [abs.]: Houston, Lunar and Planetary Institute, Lunar and Planetary Science XXV, p. 1151–1152.

Roddy, D. J., Shoemaker, E. M., and Anderson, R. R., 1994, Manson impact structure research program: Summary through February 1994, *in* Proceedings, International Symposium on the Observation of the Continental Crust through Drilling, 12th Santa Fe, April 1994: College Station, Texas, Texas A&M University, Drilling, Observation, and Sampling of the Earth's Continental Crust, p. 203–207.

Stöffler, D., and Grieve, R. A. F., 1994, Classification and nomenclature of impact metamorphic rocks: A proposal to the IUGS subcommision on the systematics of metamorphic rocks [abs.]: Houston, Lunar and Planetary Institute, Lunar and Planetary Science XXV, p. 1347–1348.

Stöffler, D., Knöll, H. -D., and Maerz, U., 1979, Terrestrial and lunar impact breccias and the classification of lunar highland rocks, *in* Proceedings, Lunar and Planetary Science Conference, 10th, Geochimica et Cosmochimica Acta, Supplement 11: New York, Pergamon Press, p. 639–675.

Witzke B. J., 1990, General stratigraphy of the Phanerozoic and Keweenawan sequence, M. G. Eischeid #1 drillhole, Carroll County, Iowa: Iowa Department of Natural Resources, Special Report Series 2, p. 39–57.

Manuscript Accepted by the Society February 22, 1995